Received: 5 October 2024 | Revised: 22 March 2025 | Accepted: 23 April 2025

DOI: 10.1111/jfb.70074

REGULAR ARTICLE

JOURNAL OF FISH BIOLOGY fsbi

Deciphering age, growth and maturity patterns in one of the smallest but data-deficient shark species, slendertail lanternshark (*Etmopterus molleri*), from the East China Sea

Mboglen David[1,2] | Narcisse Ebango Ngando[3] | Yongfu Shen[1] | Yunkai Li[1,4,5]

[1]College of Marine Living Resources Sciences and Management, Shanghai Ocean University, Shanghai, China

[2]Specialized Research Station on Marine Ecosystems, Institute of Agriculture Research for Development (IRAD), Kribi, Cameroon

[3]Department of Oceanography, Institute of Fisheries and Aquatic Sciences, University of Douala, Douala, Cameroon

[4]The Key Laboratory of Sustainable Exploitation of Oceanic Fisheries Resources, Ministry of Education, Shanghai, China

[5]National Engineering Research Centre for Oceanic Fisheries, Shanghai Ocean University, Shanghai, China

Correspondence
Yunkai Li, College of Marine Living Resources and Management, Shanghai Ocean University, Shanghai, China.
Email: ykli@shou.edu.cn

Funding information
National Natural Science Foundation of China, Grant/Award Number: #42276092; Program for Professor of Special Appointment (Eastern Scholar) at Shanghai Institutions of Higher Learning

Abstract

Deep-sea sharks represent a vulnerable group due to their unique life-history traits, including slow growth and late maturity. This study aims to fill knowledge gaps on key demographic parameters of *Etmopterus molleri*, a lanternshark species, one of the smallest shark species recorded, classified as 'data deficient' in the East China Sea. A total of 280 specimens (165 females and 115 males) were analysed to estimate age, growth and sexual maturity. Post-cranial vertebral section was treated with cobalt nitrate hexahydrate for improved age determination. Age estimation from band pair ranged from 0 to 13 in females and from 1 to 12 in males [coefficient of variation (CV) = 2.27%, average percent error (APE) = 1.60%]. The von Bertalanffy curve with the Bayesian growth Markov chain Monte-Carlo (MCMC) models using observed and back-calculated data provides the best-fit estimation compared to all models, demonstrating an asymptotic length of $L_\infty = 391.61 \pm 10.06$ mm for males and $L_\infty = 486.28 \pm 14.71$ mm for females, with a common birth size (L_0) of around 100 mm. The growth completion rates were (k) of 0.16/year for the males and 0.11/year for the females, marking sexual dimorphism, with females reaching larger sizes ($L_{50} = 287.78$ mm) and maturing later ($A_{50} = 6.57$ years) than males ($L_{50} = 260.33$ mm, $A_{50} = 4.77$ years). This maturity life strategy, typical of deep-sea elasmobranchs, underscores the vulnerability of *E. molleri*. A prudent management approach and continuous monitoring are essential for collecting more data to understand their ecology and preserve their fragile future.

KEYWORDS
Bayesian growth model, East China Sea, frequentist growth model, slendertail lanternshark, vertebral analysis

1 | INTRODUCTION

Sharks are crucial predators in marine ecosystems, exerting top-down control on trophic structures and food web dynamics (Cortés, 1999; Du et al., 2022; Heupel et al., 2014). Despite their ecological importance, many shark species are commonly caught in various commercial fisheries targeting teleost fishes (Bottari et al., 2014; Campana et al., 2016; Graça Aranha et al., 2023). Moreover, the expansion of deep-sea fisheries has led to increasingly frequent interactions with deep-water sharks as by-catch, potentially resulting in significant declines in their abundance (Dulvy et al., 2014; Finucci et al., 2021, 2024; Morato et al., 2006). This situation poses a critical challenge to the conservation of these vulnerable species, which are characterized by slow growth rates, late maturity and low fecundity (Simpfendorfer & Kyne, 2009). Particularly for deep-sea shark species, as fisheries progressively expand into deeper waters (Finucci

et al., 2024; Morato et al., 2006; O'Hea et al., 2020; Victorero et al., 2018), 14.1% of deep-sea sharks and rays are now considered endangered (Dulvy et al., 2014; Finucci et al., 2021, 2024). Typically, the deep-sea shark species are discarded due to their low value as by-catch and lack of direct economic value, masking important information about population structure, fishing vulnerability and biological traits (Gennari & Scacco, 2007; Graça Aranha et al., 2025; Rodríguez-Cabello & Sánchez, 2017). Thus, this practice impedes both population trend assessments and the development of effective management strategies and conservation for deep-sea sharks (Akhilesh et al., 2020; ICES, 2020; Myers & Worm, 2005). However, there are some notable exceptions, such as the 'landing obligation' under the Common Fisheries Policy of the European Union (Regulation EU, 2018; Regulation EU, 2021), which serves as an incentive measure aimed at reducing unwanted catches and ensuring their inclusion in fishing statistics.

The characterization of demographic information is of utmost importance in modelling the sustainability of populations under fishing pressure (Beal et al., 2022; Hilborn & Walters, 1992; Punt & Hilborn, 1997). Accurate age, growth estimates and sexual maturity are crucial input parameters for the toolbox of modelling approaches used for designing sustainable management practices and conservation strategies (Elliott et al., 2020; Melis et al., 2023; Natanson et al., 2018; Smart et al., 2016). Unfortunately, such information is not readily available for most deep-sea shark species due to logistic constraints, lack of economic value and, hence, research investment (Myers & Worm, 2005; Kyne & Simpfendorfer, 2010; Dulvy et al., 2014; Feng et al., 2022). Understanding shark's life-history traits, such as longevity, reproductive age, growth rates, is essential for evaluating their biological productivity and their ability to sustain current fishing exploitation levels (Cailliet & Goldman, 2004; Fadool et al., 2024; Francis & Ó Maolagáin, 2019; Matta et al., 2017; Pardo et al., 2013; Wong et al., 2022).

In sharks, one of the most widely employed methods for estimating age and growth is the analysis of vertebral bands and/or spines due to the absence of available otoliths or other annular structures. This approach is based on the assumption that calcified structures undergo continuous development throughout an individual's life span and serve as a permanent record of growth, exhibiting periodic patterns linked to variations in growth rate caused by environmental (biotic and abiotic) and endogenous factors, such as ontogenetic events (Burke et al., 2020; Cailliet et al., 2006; Coiraton et al., 2019; Smith et al., 2013).

Frequentist approaches are extensively used for estimating shark growth parameters modelling (Baje et al., 2018; Gervelis & Natanson, 2013; Goldman et al., 2012). For example, the von Bertalanffy growth model is widely used to model fish and shark growth based on a differential equation that describes growth as a function of size, relative growth rate and asymptotic size (Croll & van Kooten, 2022; Flinn & Midway, 2021; Kindong et al., 2020). However, these frequentist models rely on curve fitting based solely on available data. In situations where young or old specimens are scarce or absent, the models may fail to accurately capture the underlying growth curve, leading to biased estimates of growth, particularly for younger or older age classes typically, depending on which group is underrepresented in the dataset (Doll & Lauer, 2013; Smart & Grammer, 2021). Bayesian models can overcome the challenges associated with the scarcity of specimens of certain age classes by considering prior knowledge about the growth of species of interest in addition to the available data (Caltabellotta et al., 2021; Jiao et al., 2011; Smart & Grammer, 2021). Among these, the Markov chain Monte-Carlo (MCMC) method has gained increasing popularity (Kim et al., 2022; Pardo et al., 2016; Wong et al., 2022); its iterative approach allows for estimating growth parameters while taking into account prior knowledge about parameter distributions, thus enabling more robust estimates even with limited datasets.

The slendertail lanternshark (*Etmopterus molleri*) is one of the smallest deep-sea shark species, with a restricted geographic distribution encompassing the western Pacific Ocean (WPO) along New Zealand and Australia's east coast (specifically off Sydney, New South Wales) and the East China Sea (ECS) continental shelf (Ebert et al., 2013; Last & Stevens, 2009; Yano, 1988). Typically found at depths between 200 and 860 m, *E. molleri* remains poorly studied, with available data limited to basic biological parameters, including the estimated maximum total length (~460 mm), estimated male size-at-maturity (~330 mm) and size-at-birth (~150 mm) (Ebert et al., 2013; Last & Stevens, 2009). Additional research has focused on bioluminescence features (Duchatelet et al., 2019), buoyancy characteristics (Pinte et al., 2019), swimming capabilities (Pinte et al., 2020) and muscle composition and enzyme activities (Pinte et al., 2021). Due to the scarcity of information regarding its life history and population dynamics, the slendertail lanternshark is currently classified as 'data deficient' on the IUCN Red List Assessment (Kyne et al., 2015).

In the ECS, the species is caught and discarded as by-catch in deep-water trawl fisheries, the current stock status of the slendertail lanternshark in the ECS is unknown because no quantitative stock assessment has been undertaken due to its lack of commercial value. As a result, information on the slendertail lanternshark's biological parameters, including age-based characteristics, along with accompanying growth rates and life history, is still very limited in the ECS. The present study investigates the patterns of population life history of the slendertail lanternshark in the ECS, especially regarding age, growth and sexual maturity; the aims of this study are to (1) estimate the age of *E. molleri* specimens by examining growth band pair counts in vertebral centra, (2) compare age-enhancement techniques to determine the most effective method for assessing age in poorly calcified structures, (3) generate and compare the best growth models for this species using both frequentist and Bayesian approaches and (4) determine ages at sexual maturity for both sexes based on macroscopic analysis.

2 | MATERIALS AND METHODS

2.1 | Sampling

E. molleri specimens were collected between January and April 2023 as by-catch from commercial vessels operating on the ECS continental

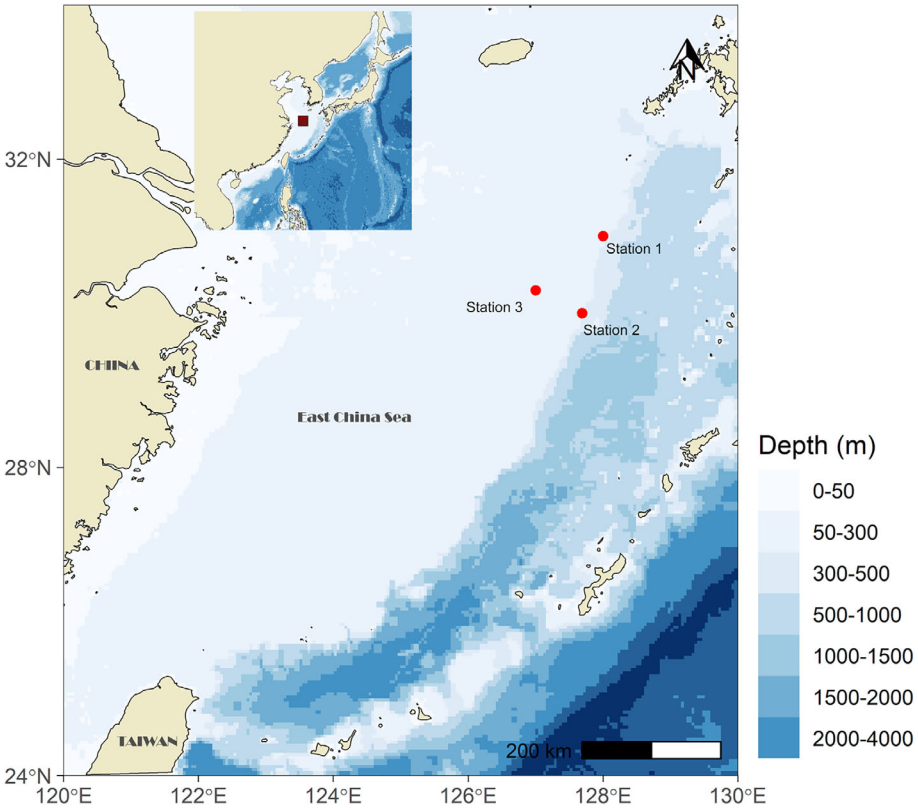

FIGURE 1 Collection map of the sampled slendertail lanternshark; red dots represent sampling stations.

shelf. Specimens were captured through bottom trawl fishing at three sampling stations (station 1: 30° 36′37 N–128°10′49 E; station: 2 29°47′29 N–127°47′46 E; station 3: 30°7′20 N–127°28′43 E; Figure 1) at depths of 300–400 m, using nets with a codend mesh-size of 40 mm primarily targeting demersal species. After each trawl, shark samples were labelled and stored at −20°C for further analysis. In the laboratory, after defrosting, sharks were visually identified based on external morphology and colouration using the identification key revised by Ebert and Van Hees (2018), and muscle tissue samples were also collected for subsequent DNA analysis to confirm visual identifications. Immediately after the identification, their total length (TL, cm; ± 0.1 cm), total weight (TW, g; ± 0.1 g), eviscerated weight (EW, g; ± 0.1 g), sex and maturity stage were recorded as described below.

2.2 | Sex ratio and length-weight relationship

Sex ratio (females: males) was assessed for the total number of specimens and compared with the 1:1 ratio using the χ^2 test (Zar, 1999). The length-weight relationships were obtained using power regression (exponential curve) based on Equation (1) (Pauly, 1983): $EW = aTL^b$ modified, where EW is the eviscerate weight (g) of fish, TL is the total length (mm) of fish, a (intercept) describes the rate of change of weight with length and b the slope of the regression. The values of the constants a and b were estimated using linear regression model based on the logarithmic form of Equation (2): Log (EW) = Log. a + b.Log(TL). When the slope b is equal to 3, isometric pattern of growth occurs, but when b is not equal to 3, allometric pattern of growth occurs, which may be positive if >3 or negative if <3. The slope b of the regressions was tested against the isometric slope standard of 3 by sex and overall with Student's *t*-test function (Pauly, 1983). Additionally, the analysis of covariance (ANCOVA) test was used to investigate sex differences on the aforementioned relationship. Regression analysis and statistical tests were performed using the R version 4.3.2 (2023-10-31 ucrt).

2.3 | Sexual maturity and reproductive metrics

Direct macroscopic examination of gonads allowed sex determination. Then, maturity status was assigned using previously established criteria for aplacental and placental viviparous sharks (Coelho & Erzini, 2007; Stehmann, 2002), supplemented by Wu et al. (2020) and Kousteni (2021). For the males, assessment focused on the length and rigidity of the clasper, condition of the testes and sperm sacs, presence of sperm in the genital tract and classified on four maturity life stages: stage I (immature), stage II (maturing), stage III (mature) and stage IV (active). Females were classified using a seven-stage maturity scale based on the condition of their ovaries and uteri (size and colour of the ovaries, uteri containing large eggs, presence of embryos inside the uteri and the developmental stage of embryos): stage I (immature), stage II (maturing), stage III (mature), stage IV (early pregnancy), stage V (middle pregnancy), stage VI (expecting) and stage VII (post-natal) (Table 1). Expressed as a binary score (immature/maturing = 0 and mature or beyond = 1), these data were used to determine the size

TABLE 1 Maturity stage classification for placental viviparous sharks, used for characterizing the maturity stage of *Etmopterus molleri* (binary score: 0 = immature and maturing; 1 = mature or sexually active).

Maturity stages	Males	Females	Binary score
Stage I	Claspers undeveloped as small, flexible sticks being shorter than extreme tips of posterior pelvic-fin lobes	Ovaries small or invisible, internal structure gelatinous or granulated, no oocytes differentiated. Uteri thread-like. No uterine egg cases	0
Stage II	Claspers becoming extended, longer than tips of posterior pelvic-fin lobes, skeleton still soft and flexible	Mildly enlarged ovaries with more translucent walls. Oocytes becoming differentiated to various small sizes. No uterine egg cases	
Stage III	Claspers fully formed and stiff, spines of glans free and sharp, with free cartilaginous spines mostly erect	Ovaries large, well rounded. Oocytes obviously enlarged, all to about the same size, can easily be counted and measured	1
Stage IV	The clasper glans is often dilated and swollen, cartilaginous spines mostly erect; sperm flows from the cloaca under pressure into the seminal vesicle and/or is present in the clasper groove	Uteri well filled and rounded with seemingly unsegmented yolk content	1
Stage V		Uteri well filled and rounded with segmented content of large yolk balls, can easily be counted and measured + embryos are variously small, unpigmented, atop their yolk balls and larger ones with external gill filaments	1
Stage VI		Embryos formed, pigmented, external gill filaments lost and yolk sacs obviously reduced. It can be counted, measured and sexed easily.	1
Stage VII		Ovaries at resting and uteri are empty but remain dilated along their entire length, in contrast to the other stages.	1

and age at maturity. Furthermore, uterine fecundity was estimated using an embryo count or number of fertilized eggs present in each uterus. The largest oocytes in the ovary were also counted to estimate ovarian fecundity (Pratt, 1979). The total length and sex of each embryo were measured, and size at birth was estimated using the size of the largest embryo and the smallest neonate capture at the same time and place.

2.4 | Age and growth

For each specimen, a set of 5–7 vertebrae were removed between the cranium and the first dorsal fin, separated into individual centra and stored frozen for subsequent age determination. Vertebrae processing and ageing followed protocols described by Cailliet et al. (2006). After defrosting, any unnecessary tissue was removed from the vertebrae using a scalpel. For complete cleaning of residual tissues, vertebrae were soaked in 5% sodium hypochlorite solution (commercial bleach) for 2–3 min depending on vertebrae size and then rinsed with distilled water for a few minutes and stored in ethanol at 75%.

These centra were then air-dried for approximately 25 min before staining. Two staining processes were tested to identify the most effective solution for distinguishing growth bands. First, whole centra were stained with a 5% cobalt nitrate hexahydrate solution according to the method proposed by Hoenig and Brown (1988) and modified by Gennari and Scacco (2007). The second stain used was 0.01% alizarin red S solution 12 (Jolly et al., 2013). The effectiveness of these different staining procedures in determining the readability of growth band pairs across the entire vertebral centra was compared.

After staining, the centra were mounted on a microscope slide and observed under both refraction and transmitted light using an Olympus DP71 stereomicroscope and digital camera at 10–40× magnification, depending on the vertebrae size. Digital images of processed vertebrae were captured and growth bands counted and marked after enhancing images using Adobe Photoshop (version 23.2.0). Growth band pairs were defined as a succession of a translucent band and an opaque band along a transect from the centrum radius to the outer edge (year of capture). Although samples did not cover a wide range of capture periods for formal marginal increment analysis, annual growth band deposition was assumed, consistent with validated ageing techniques for closely related species such as *Etmopterus spinax* and *Etmopterus baxteri* (Coelho & Erzini, 2008b; Irvine et al., 2006).

All vertebral centra were examined independently by two readers without knowledge of sex and length. Growth band pair counts were directly accepted only if both readings were in agreement. If counts differed by one band pair, centra were recounted, with the final count (estimated age = EA) accepted if matching one previous count or rejected otherwise. Only vertebrae whose band pair counts obtained two out of three equal readings were considered for the age and growth analysis. Precision and error analyses were assessed using the average percent error (APE) and the average coefficient of variation (ACV). McNemar's test, the Evans-Hoenig's test and Bowker's symmetry test was used to estimate bias between readers.

TABLE 2 Equations of the three growth functions used in the frequentist approach.

Model	Growth functions
3-VBGF	$L_{(t)} = L_0(L_\infty - L_0)(1 - \exp(-kt))$
Log	$L_{(t)} = \frac{L_\infty L_0(\exp(gt))}{L_\infty + L_0(\exp(gt) - 1)}$
Gom	$L_{(t)} = L_0 \exp\left(\ln\left(\frac{L_\infty}{L_0}\right)\right)(1 - \exp(-gt))$

Note: $L_{(t)}$ is the predicted length at age t; L_∞ is the asymptotic or theoretical maximum mean length at $t = \infty$; $L_{(0)}$ is the length at birth; and k and g are the growth completion rates.
Abbreviations: Gom, Gompertz growth function; Log, logistic growth model; VBGF, von Bertalanffy growth model.

The lengths-at-previous-ages for each individual sample were estimated by back-calculation techniques, as it's the first time to evaluate growth history for this species, and the sample period was limited (Cailliet & Goldman, 2004). To do that, the centrum radius (Cr), the distance to the birthmark and the distance to each growth band pair were measured to the nearest 1 μm. Based on the relationship between Cr and total length, our back-calculation models were performed: the Dahl-Lee direct proportions model (DALE), the Biological Intercept Fraser Lee model (BI), the Quadratic Scale Proportional Hypothesis (QSPH) model and the Quadratic Body Proportional Hypothesis (QBPH) model. Accuracy, error analysis and age-bias plot and back-calculation model were perform using the 'FSA' package version 0.9.5 and 'RFishBC' package version 0.2.7 (Ogle, 2023; Ogle et al., 2023) in the R version 4.3.2 (2023-10-31 ucrt). We performed an analysis of variance (ANOVA) test using model output parameters (L_o and L_∞), observed sizes and back-calculated mean sizes to assess differences in size parameters between males and females.

2.5 | Growth model fitting and statistical analysis

Age and TL (in mm) data were used to estimate growth parameters by applying two model-fitting approaches.

2.5.1 | Frequentist approach

Three deterministic growth models were fitted to the observed length-at-age data following Cailliet et al. (2006): (1) von Bertalanffy's growth model (VBGF), (2) logistic growth model (Log) and (3) Gompertz growth function (Gom) (Table 2). Last and Stevens (2009) and Ebert et al. (2013) estimated the size at birth of *E. molleri* to be approximately 150 mm off the Australian coasts. However, the present study recorded a minimum size of 106.5 mm, indicating a closer resemblance to a neonate. Furthermore, a fully formed embryo of size $L_{embryon} = 87.5$ mm without yolk sac was found in a pregnant female. Two approaches were used for the VBGF models: (1) standard three-parameter growth models (3-VBGF), (2) versions of the growth models (2-VBGF), with three hypothetical lengths at birth ($L_0 = 106.5$ mm corresponding to the minimum size found in our samples, $L_0 = 95$ mm represents the average length between L_0 and $L_{embryon}$ and L_0 from the back-calculated data) to provide reference points for the models given the size class of individuals aged 0 years. Separate growth models were constructed for males, females and combined sexes. Growth models were fit using non-linear least squares (nls) function using the 'Estimate_Growth' function within the 'AquaticLifeHistory' version 1.0.5′ R package (Smart et al., 2016). The model with the lowest corrected Akaike's Information Criterion (AICc) value was chosen as the best fit for the data.

2.5.2 | Bayesian approach

A Bayesian approach utilizing MCMC simulation was implemented to address some of the inherent shortcomings in frequentist growth models. Informative priors were specified for the models, including L_∞ and L_0 as normal distributions with means and standard errors (SE). The growth coefficients (k_{max}/g_{max}) and sigma (σ) values were assigned uniform priors with specified upper and lower limits, and the growth curve displayed a normal error structure (Smart & Grammer, 2021). The prior length-at-birth used to fix the MCMC model was set at $L_0 = 95 \pm 3.15$ mm and maximum size $L_\infty = 389.1$ mm (the maximum length observed in the samples studied), assuming that was the largest size likely to be found in the study area. Then two theorical maximum lengths were chosen to simulate the probable evolution of the maximum size based on the back-calculated data for each sex (Table 3).

The growth completion rates ($k_{max} = 1$ for VBGF, $g_{max} = 1$ for Gompertz and Log models) and sigma values ($\sigma_{max} = 100$) were uniform priors with upper and lower bounds, and the growth curve followed a normal error structure (Smart & Grammer, 2021).

The evaluation of the different Bayesian models was conducted using the 'Estimate_MCMC_Growth' function from the 'BayesGrowth' R package version 1.0.0 (Smart & Grammer, 2021). We ran four MCMC chain with 10,000 iterations to estimate the posterior distributions of the parameters with a burn-in period of 5000 iterations. We confirm algorithm convergence using the Gelman-Rubin test [$\hat{R} = (1–1.05)$] for all models and traceplots for the autocorrelation for the best MCMC growth model. The selection of the best Bayesian model was based on the leave-one-out cross-validation information criterion (LOOIC), with the retained model being the one with the lowest LOOIC value (Hooten & Hobbs, 2015).

The length-at-maturity was estimated for both sexes using the 'Estimate_Len_Maturity' function from the 'AquaticLifeHistory' package in R. This function fits a logistic regression model to maturity data (binary 0/1) with binomial errors based on length. The lengths at which 50% (L_{50}) and 95% (L_{95}) of individuals reach maturity, along with their associated confidence intervals, were calculated. Similarly, age-at-maturity was estimated using the 'Estimate_age_maturity' function, which employs a similar logistic regression approach on age-maturity data. This provided estimates of the ages at which 50% (A_{50})

TABLE 3 Summary of prior information for setting the Markov chain Monte-Carlo (MCMC) model.

Prior information		Males	Females
Theorical size-at-birth	Expected	$L_0 = 95 \pm 3.15$ mm	$L_0 = 95 \pm 3.15$ mm
	Back-calculated	$L_0 = 101.50 \pm 2.23$ mm	$L_0 = 104 \pm 1.43$ mm
Theorical max length (from best frequentist model)	Observed data	$L_{max} = 398.1 \pm 3.15$ mm	$L_{max} = 398.1 \pm 3.15$ mm
	Back-calculated	$L_{max} = 418 \pm 13.47$ mm	$L_{max} = 526 \pm 17.72$ mm

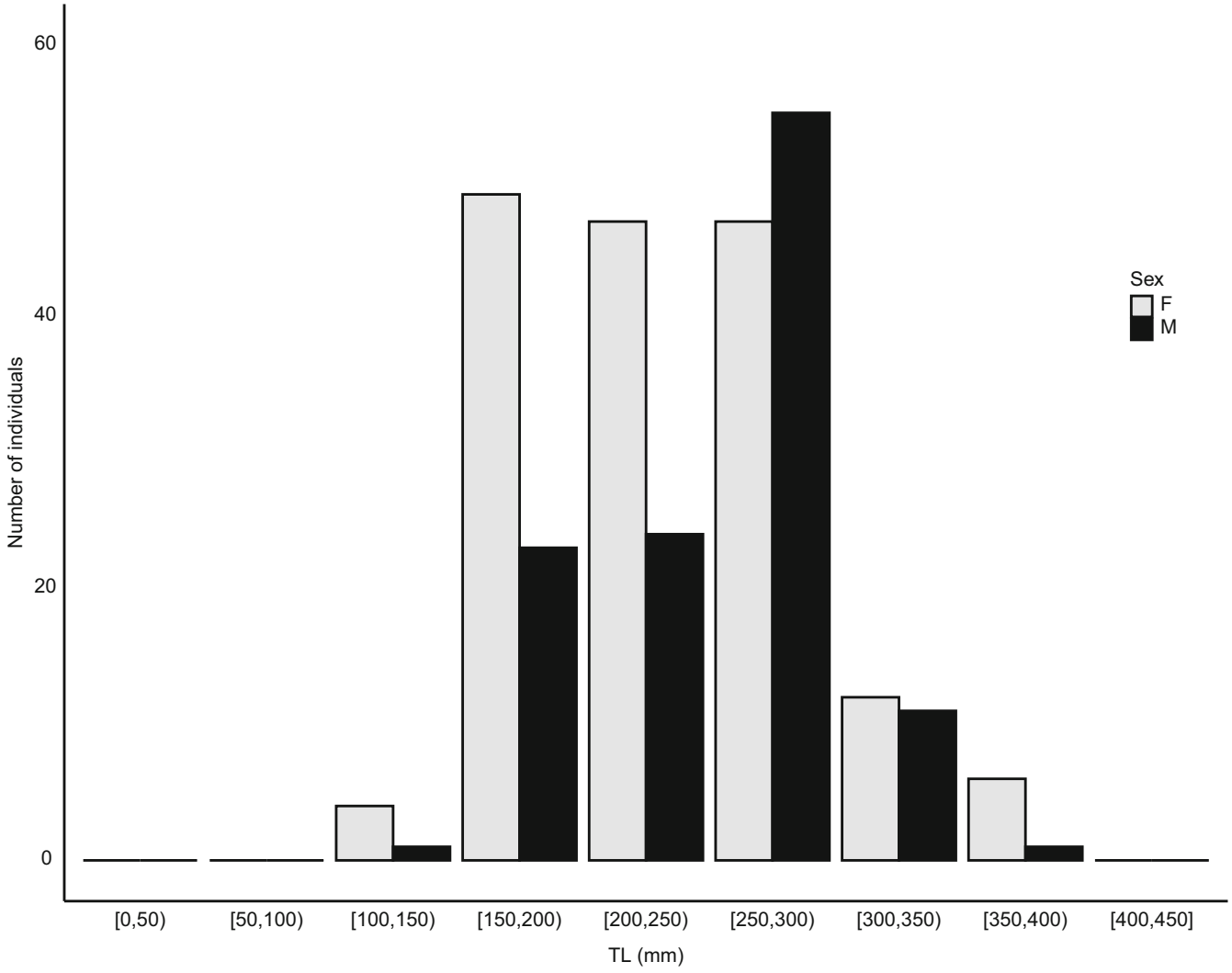

FIGURE 2 Length class distribution of male and female *Etmopterus molleri* samples from the East China Sea (ECS).

and 95% (A_{95}) of individuals reach maturity for each sex, along with corresponding confidence intervals.

3 | RESULTS

3.1 | Sample characteristics

A total of 280 *E. molleri* specimens (165 females and 115 males) were collected and analysed in this study. Immature individuals made up nearly 70% of the samples, with a sex ratio of 1.43:1 favouring females ($\chi^2 = 146.52$, $p < 0.01$); this finding indicates significant imbalance in the sex-based distribution. The length distribution ranged from 106.5 to 389.1 mm for females and 121.5–371.1 mm for males (Figure 2, Supplementary Materials S2). No difference was observed in the slope regarding the TL-EW relationship between the different sexes (Figure 3), and *t*-test showed that $b = 3.032$ (b of combined sex) is not significantly different from $b = 3$ (*t*-test, $p > 0.05$, $df = 279$), indicating an isometric growth pattern. The ANCOVA model revealed a highly significant effect of sex on the length

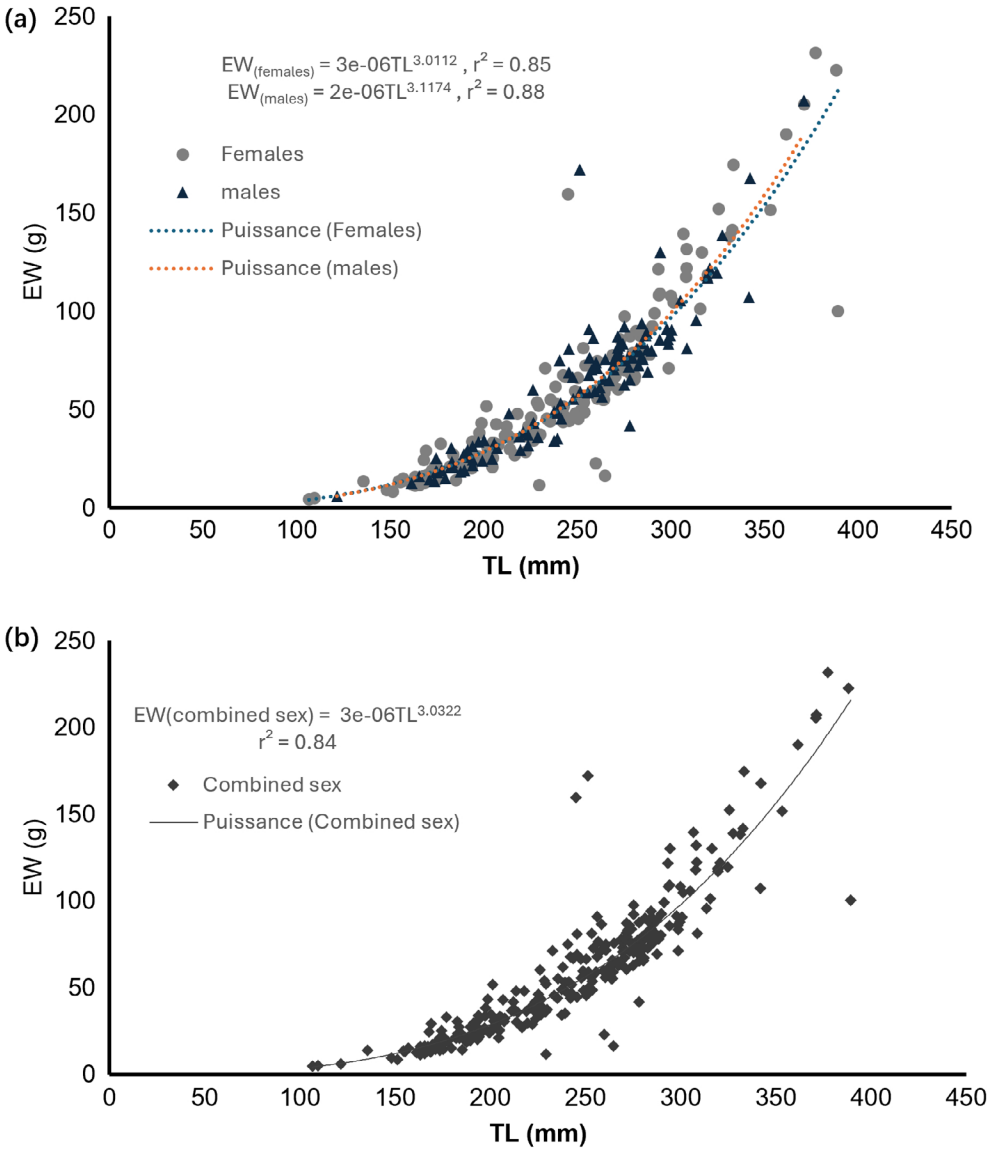

FIGURE 3 Total length (TL) and eviscerated weight (EW) relationship between (a) males ($n = 115$) and females ($n = 165$) and (b) combined sex of *Etmopterus molleri* caught in the East China Sea (ECS).

($F_{1266} = 1109.133$, $p < 0.05$), with females generally larger than males.

Among the specimens analysed, various maturity stages were recorded, with most individuals, regardless of sex, being in the immature stage. Of the 165 females examined, 109 were immature at stage I (66.05%), 21 were immature at stage II (12.73%), 19 were at stage III (11.52%), 15 were at stage V (9.10%) and 1 individual was at stage VI. Among male specimens, 36 were immature at stage I (31.30%), 20 were transitioning to maturity at stage II (17.39%) and 59 were mature at stage III (51.30%). At stage VI, a gravid female (351.4 mm TL) revealed a single female embryo measuring 87.5 mm TL. However, this observation was insufficient to draw conclusions regarding the fecundity of the species.

Ovarian fecundity analysis revealed 1–9 ripe oocytes per female, with a mean value of 6.33 ± 2.06. The modal count was seven ripe oocytes ($N = 4$ females), whereas the maximum count of nine ripe oocytes was observed in two specimens. Examination of 15 females yielded measurements for 95 oocytes, comprising 17 ripe, 31 maturing and 47 immature specimens. Eight females had oocytes with a maximum diameter ranging from 20 to 25 mm, whereas two females had oocytes measuring between 27 and 30 mm (Supplementary Materials S1).

3.2 | Stain evaluation and selection

The effectiveness of the staining methods was evaluated by directly observing the growth bands on whole vertebrae under a microscope. The cobalt nitrate hexahydrate staining (Figure 4a,c) allowed for better age determination compared to alizarin red S (Figure 4b,d). Consequently, vertebrae stained with cobalt nitrate hexahydrate were selected for age reading and estimation (Figure 4e).

3.3 | Age determination

A total of 280 samples of vertebral centrum stained with cobalt nitrate hexahydrate were observed and read by two (if necessary

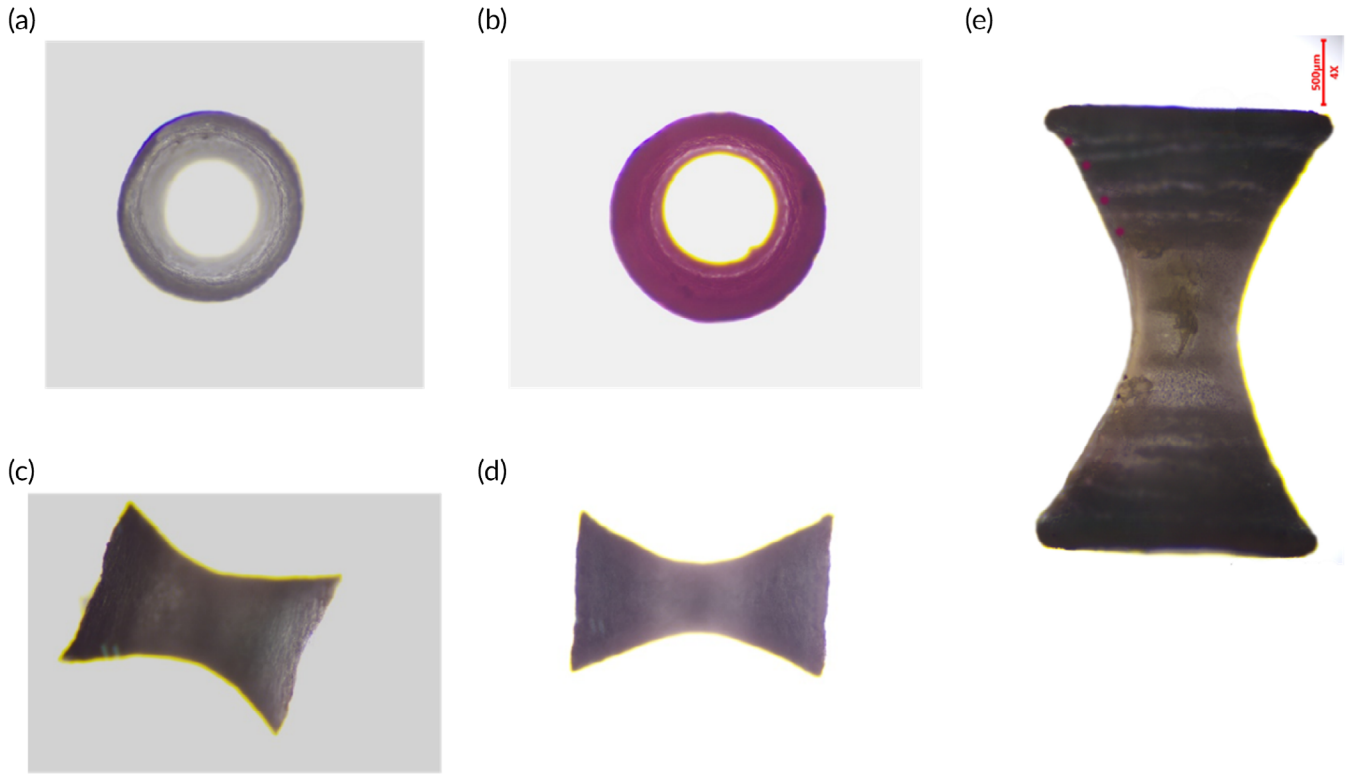

FIGURE 4 Images of *Etmopterus molleri* vertebrae stained with cobalt nitrate hexahydrate (a = top view, c = side view, for a 1-year-old specimen) and alizarin red S (b = top view, d = side view, for a 1-year-old specimen); (e) a 4-year-old specimen stained with cobalt nitrate hexahydrate.

three) readers. Band pair counts were based on the corpus calcareum, and 234 samples met the requirements (the same reading from at least two readers). Age estimates ranged from 0 to13 for females (TL: 106.5–389.1 mm) and 1 to 12 for males (TL: 121.5–371.1 mm). The CV and APE between readings were 2.27% and 1.60%, respectively, signifying high reproducibility in the age determination between the readers (Figure 5). McNemar's test and Evans-Hoenig's symmetry test were significant ($p < 0.05$), indicating asymmetry in the contingency, but the Bowker test was not significant ($df = 10$, $\chi^2 = 8.50$, $p > 0.05$), suggesting that the observed asymmetry could be due to chance, and that disagreements between readers may be considered balanced overall (Supplementary Material S3).

3.4 | Growth models

The relationship between Cr and TL for both males and females was non-linear and best explained by the quadratic QBPH model (Supplementary Material S4), which exhibited the smallest deviation from the observed data. Although the estimated size at birth was similar for both sexes (108 ± 2.1 mm), the back-calculated size data revealed a significant difference between males and females as growth progressed (ANCOVA, $F_{1,1263} = 14.69$, $p < 0.05$); therefore, sex-specific growth modelling was conducted.

Using a frequentist approach, the VBGF growth model with back-calculated data provided a more accurate estimation of the growth parameters for *E. molleri* in both males and females. For males, the estimated parameters were $L_0 = 101.57 \pm 2.23$ mm for size at birth and $L_\infty = 418 \pm 13.47$ mm for asymptotic length. For females, size at birth was estimated at $L_0 = 104.50 \pm 1.43$ mm, with an asymptotic length of $L_\infty = 526 \pm 17.72$ mm.

Based on the observed data, the standard VBGF growth model with hypothesis 3 (L_0 set at 95 mm) had the best parameters (low AICc and $w = 1$) for males and was used to describe the mean asymptotic length ($L_\infty = 371.07 \pm 9.43$ mm). Similarly, the standard VBGF growth model for females (L_0 set at 106.5 mm) had the lowest AICc, $w = 1$, and was selected to express the mean asymptotic length ($L_\infty = 472.12 \pm 15.69$ mm) (Table 4).

It is worth noting that for both sexes, the growth models derived from back-calculated data and observed data converged in terms of birth sizes ($F = 0.342$, $p = 0.38$) and were close to the minimum observed size; however, they differed in asymptotic lengths, particularly for males (Figure 6).

The Bayesian VBGF model provided the most robust growth parameter estimates for both sexes. In males, the three hypotheses showed no significant differences (ΔLooic <2), with estimated birth lengths ranging from 96.40 ± 3.02 mm to 101.88 ± 2.12 mm and asymptotic lengths varying between 396.43 ± 2.87 mm and 391.61 ± 10.06 mm. Similarly, for females, the Bayesian VBGF model yielded optimal growth parameter estimates, with birth lengths ranging from 93.52 ± 2.39 mm to 105.35 ± 1.33 mm and asymptotic lengths spanning from 401.21 ± 2.97 mm to 496.49 ± 13.75 mm (Table 5).

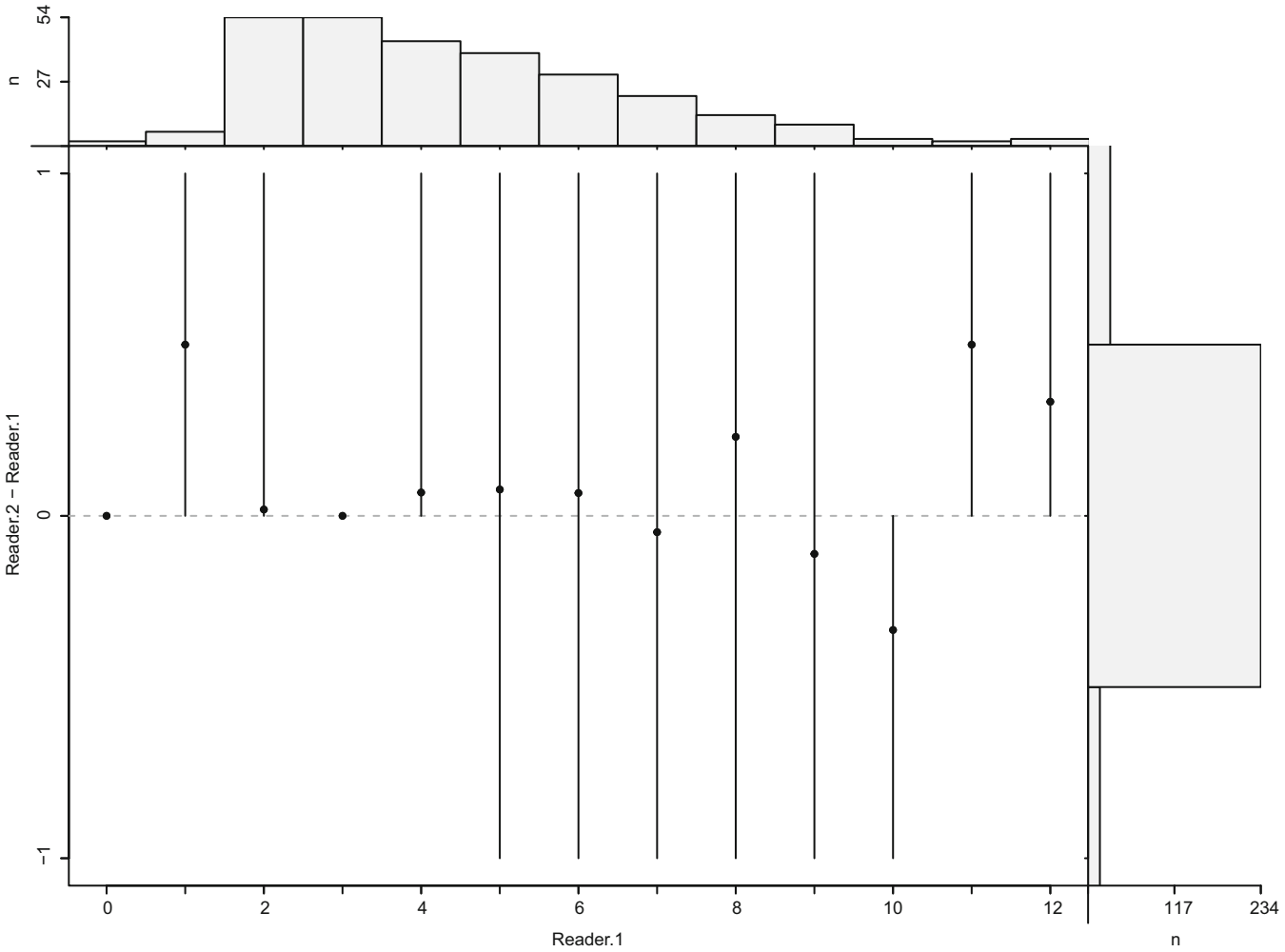

FIGURE 5 Age-bias plot of reader 1 estimates versus reader 2 estimates. Mean (points) and range (intervals) of differences in age estimates obtained from *Etmopterus molleri* vertebrae between the two readers at the estimates for the first reader. The agreement line (horizontal dashed grey line) refers to the difference in the two age estimates from readers. The marginal histograms depict the age estimates of the first reader (top) and the differences between the age estimates between readers (right), and the bar at a difference of zero represents the amount of perfect agreement between the sets of age estimates ($n = 234$).

Growth parameter estimates from both best-fit models (frequentist and Bayesian) exhibited similar birth lengths for males and females. Asymptotic lengths, on the contrary, showed differences. The Bayesian model gave much more accurate estimates than the frequentist approach (Figure 7).

3.5 | Length and age-at-maturity

The estimates of maturity for males and females differed substantially [multivariate analysis of variance (MANOVA, Wilks' lambda: $\lambda = 0.8349$, F_2, $87 = 8.604$, $p < 0.05$)], with females exhibiting larger sizes than males, and males displaying earlier maturity in terms of length and age. The smallest mature male specimen measured 257.5 mm and was 5 years old, whereas the largest immature specimen measured 271.3 mm and was 6 years old. Among females, the smallest mature specimen measured 272.8 mm and was 6 years old, whereas the largest immature specimen measured 280.5 mm and was 6 years old.

The mean parameters for length at 50% and 95% maturity (L_{50} and L_{95}) for males were 261.28 ± 2.22 mm TL (70.41% of the maximum observed size) and 275.84 ± 3.86 mm TL, whereas for females, they were 287.78 ± 4.19 mm TL (73.96% of the maximum observed size) and 320.44 ± 9.61 mm TL, respectively, for L_{50} and L_{95} (Table 6; Figure 8). The mean ages at 50% and 95% maturity (A_{50} and A_{95}) for males were 4.77 ± 0.16 years (39.75% of the maximum age observed) and 6.12 ± 0.32 years, respectively, whereas for females, they were 6.57 ± 0.18 years (50.54% of the maximum age observed) and 7.62 ± 0.31 years, respectively for A_{50} and A_{95} (Table 6; Figure 8 and Supplementary Material S5).

TABLE 4 Summary of results of the observed length-at-age and back-calculated data for males and females from the frequentist models incorporating corrected Akaike's Information Criterion (AICc).

	Models	*N*	AICc	*w*	L_0 ± SE (mm)	L_∞ ± SE (mm)	*k* ± SE	g_{Gom} ± SE	g_{log} ± SE	RSE
Observed data (males)										
Hypothesis 1	VBGF	**115**	**928.17**	**0.94**	**85.10 ± 10.91**	**360.44 ± 12.66**	**0.21 ± 0.03**			**13.36**
L_0 = Null	Logistic	115	939.73	0.00	118.57 ± 5.93	335.94 ± 7.68			0.38 ± 0.03	14.07
L_∞ = Null	Gompertz	115	933.89	0.05	106.60 ± 7.28	345.01 ± 9.34		0.29 ± 0.03		13.71
Hypothesis 2	VBGF	115	929.85	0.72	106.5 ± 3.15	387.51 ± 12.17	0.16 ± 0.02			13.54
L_0 = 106.5	Logistic	115	931.74	0.00	106.5 ± 3.15	324.91 ± 4.41			0.44 ± 0.03	14.20
L_∞ = Null	Gompertz	115	940.81	0.28	106.5 ± 3.15	344.91 ± 6.22		0.29 ± 0.04		13.65
Hypothesis 3	VBGF	**115**	**926.8**	**0.97**	**95 ± 3.15**	**371.07 ± 9.43**	**0.17 ± 0.01**			**13.36**
L_0 = 95	Logistic	115	933.80	0.00	95 ± 3.15	316.67 ± 3.83		0.34 ± 0.02		14.73
L_∞ = Null	Gompertz	115	949.28	0.03	95 ± 3.15	334.39 ± 5.14			0.51 ± 0.02	13.77
Back-calculated data (males)										
	VBGF	**526**	**4514.95**	**0.99**	**101.57 ± 2.23**	**418 ± 13.47**	**0.13 ± 0.01**			**13.38**
L_0 = Null	Logistic	526	4542.81	0.00	114.85 ± 1.52	344.28 ± 4.82			0.36 ± 0.01	13.71
L_∞ = Null	Gompertz	526	4524.84	0.01	109.49 ± 1.75	366.86 ± 6.89		0.24 ± 0.01		13.49
Observed data (females)										
Hypothesis 1	VBGF	**165**	**1293.38**	**1**	**104.26 ± 4.46**	**463.40 ± 21.76**	**0.11 ± 0.01**			**11.92**
L_0 = Null	Logistic	165	1303.47	0	123.86 ± 3.07	384.26 ± 8.87			0.29 ± 0.02	12.86
L_∞ = Null	Gompertz	165	1317.13	0	115.55 ± 3.54	406.52 ± 11.77		0.21 ± 0.01		12.32
Hypothesis 2	VBGF	**165**	**1291.53**	**1**	**106.5 ± 3.15**	**472.12 ± 15.69**	**0.11 ± 0.02**			**11.97**
L_0 = 106.5	Logistic	165	1307.05	0	106.5 ± 315	353.72 ± 4.67			0.39 ± 0.02	13.82
L_∞ = Null	Gompertz	165	1339.12	0	106.5 ± 3.15	386.43 ± 6.60		0.24 ± 0.03		12.54
Hypothesis 3	VBGF	**165**	**1295.2**	**1**	**95 ± 3.15**	**434.41 ± 11.17**	**0.13 ± 0.02**			**12.10**
L_0 = 95	Logistic	165	1327.73	0	95 ± 3.15	339.25 ± 4.19			0.45 ± 0.01	15.31
L_∞ = Null	Gompertz	165	1372.74	0	95 ± 3.15	367.16 ± 5.547		0.28 ± 0.02		13.36
Back-calculated data (females)										
	VBGF	**703**	**5439.79**	**1**	**104.50 ± 1.43**	**526 ± 17.72**	**0.09 ± 0.01**			**11.54**
L_0 = Null	Logistic	703	5497.51	0	117.34 ± 1.02	390.13 ± 4.74			0.30 ± 0.01	12.03
L_∞ = Null	Gompertz	703	5458.48	0	112.03 ± 1.15	425.26 ± 7.12		0.18 ± 0.01		11.701

Note: The best-fitting frequentist model is indicated in bold.

Abbreviations: AICc, small-sample bias adjusted from the Akaike's information criteria; g_{Gom}, growth parameters for Gompertz function; g_{log}, growth parameters for logistic function; *k*, the growth completion rate in year^{-1} for the VBGF; L_0 ± SE, length-at-birth ± standard error (mm, TL); L_∞ ± SE, maximum asymptotic length ± standard error (mm, TL); *n*, number of sample; RSE, residual error for the models; VBGF, von Bertalanffy's growth model; *w*, AIC_C weights.

4 | DISCUSSION

Despite the growing interest in chondrichthyans, particularly sharks, most of the available data on small sharks in deep-sea ecosystems stem from incidental catch surveys associated with the expansion of deep-sea fisheries (Victorero et al., 2018). Although reliance on this type of catch may limit comprehensive sampling, it provides an opportunity to explore resources that are otherwise difficult to access and often economically unviable (Ruibal Núñez et al., 2018; Xu et al., 2022) The specimens of *E. molleri* studied here, obtained from by-catch in the ECS, offer valuable new insights into the key life-history parameters of this poorly known and under-studied deep-sea shark species.

4.1 | Sex ratio and length distributions

The study found significant difference between the proportions of males and females in shallow depths (300–400 m) and revealed higher proportion of immature individuals. Similar trends on other small deep-water shark species were also reported in previous studies (Braccini & Taylor, 2016; Moura et al., 2014; Rodríguez-Cabello et al., 2018; Yano, 1988). For example, *E. molleri* congener *E. spinax* and *Etmopterus pusillus* catch in the shallow water of the Mediterranean Sea display over 90% and 80%, respectively, of immature individuals on both sexes (Coelho & Erzini, 2008a; Porcu et al., 2014). This observation may be related to sex segregation or maturity stage and requires more precise information for this species. The

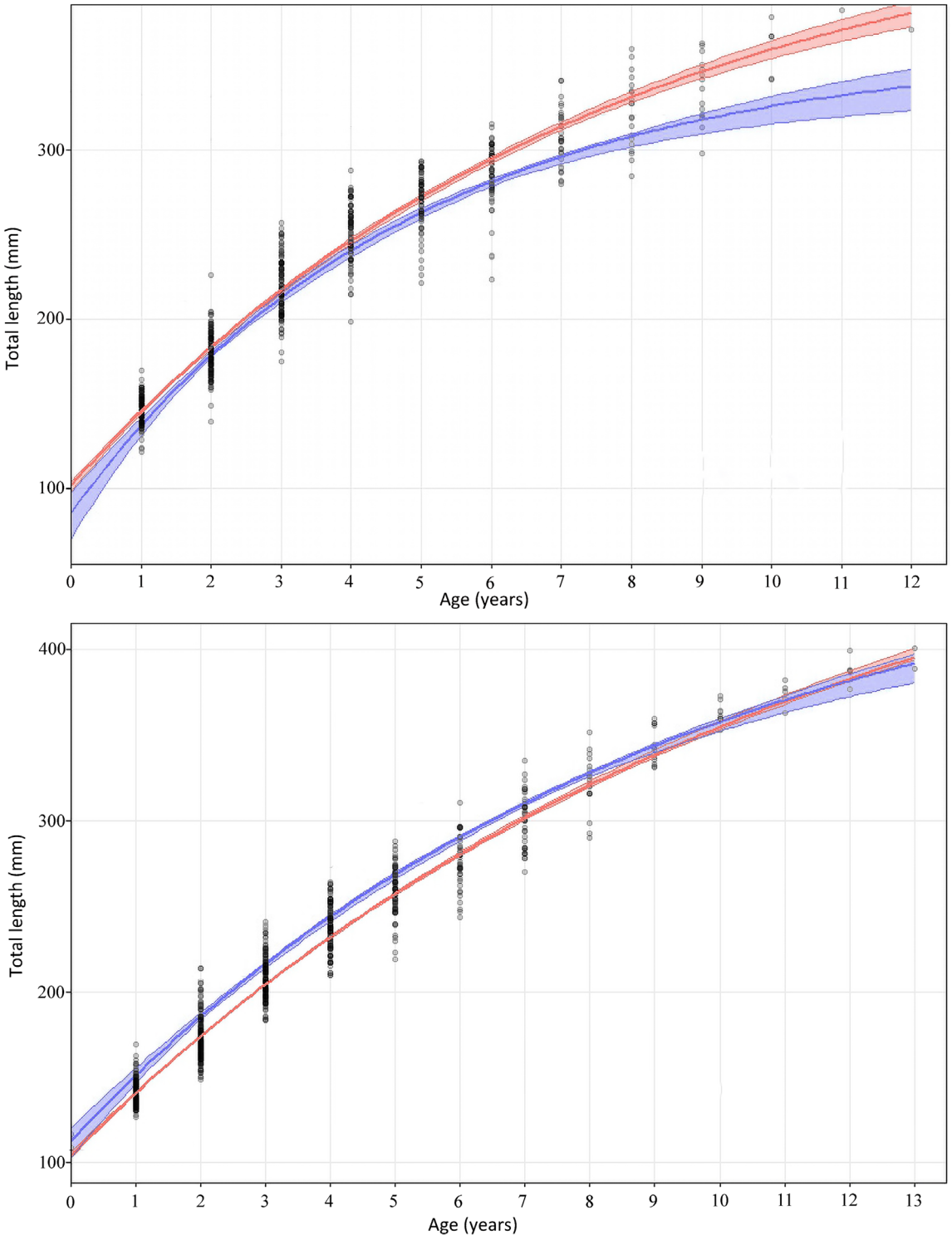

FIGURE 6 *Etmopterus molleri* growth curve in the East China Sea (ECS). (a) Males best-fitting frequentist von Bertalanffy's growth model (VBGF) model (red) with back-calculated data ($L_0 = 101.57 \pm 2.23$ mm, $L_\infty = 418 \pm 13.47$ mm, $k = 0.13$) + best-fitting frequentist model VBGF (blue) with observed data ($L_0 = 95 \pm 3.15$ mm, $L_\infty = 371.07 \pm 9.43$ mm, $k = 0.17$). (b) Females best-fitting frequentist VBGF model (red) with back-calculated data ($L_0 = 104.50 \pm 1.43$ mm, $L_\infty = 526 \pm 17.72$ mm, $k = 0.09$) + best-fitting frequentist model VBGF (blue) with observed data ($L_0 = 106.5 \pm 3.15$ mm, $L_\infty = 472.12 \pm 15.69$ mm, $k = 0.11$).

predominance of immature specimens in catches may reflect both natural population demographics, where juveniles typically constitute most viable populations, and spatial–temporal sampling bias related to sex-specific segregation patterns, maturity stages and the intensive demersal trawling activities in areas potentially serving as juvenile habitats (Du et al., 2022; Zhang et al., 2016). Otherwise, size-selective

TABLE 5 Summary of results of the observed length-at-age and back-calculated data for males and females from the Bayesian Markov chain Monte-Carlo (MCMC) model incorporating the leave-one-out cross-validation information criterion (LOOIC).

Models	Models	*n*	LOOIC ± SE	W_{LOOIC}	L_0 ± SE (mm)	L_∞ ± SE (mm)	*k* ± SE	g_{Gom} ± SE	g_{log} ± SE	Sigma
Observed data (males)										
Hypothesis 1	VBGF	**115**	**2234.90 ± 29.66**	**1**	**96.40 ± 3.02**	**391.61 ± 10.06**	**0.16 ± 0.01**			**13.67**
$L_0 = 95$	Logistic	115	2287.65 ± 32.56	0	102.41 ± 2.96	333.38 ± 5.94			0.44	14.91
$L_\infty = 418 \pm 13.47$	Gompertz	115	2258.31 ± 31.03	0	100.03 ± 3.01	354.45 ± 7.92		0.29		14.25
Hypothesis 2	VBGF	**115**	**2235.29 ± 29.65**	**1**	**96.91 ± 2.41**	**396.43 ± 2.87**	**0.16 ± 0.004**			**13.74**
$L_0 = 95 \pm 3.15$	Logistic	115	2303.99 ± 28.45	0	109.94 ± 2.88	392.15 ± 3.27			0.32 ± 0.01	19.40
$L_\infty = 398.1 \pm 3.15$	Gompertz	115	2261.87 ± 29.99	0	105.11 ± 2.80	393.36 ± 3.16		0.23		16.04
Back-calculated priors (males)										
Hypothesis 3	VBGF	**115**	**2233.80 ± 29.19**	**1**	**101.88 ± 2.12**	**397.70 ± 10.21**	**0.15 ± 0.01**			**13.70**
$L_0 = 101.57 \pm 2.23$	Logistic	115	2288.90 ± 32.72	0	105.16 ± 1.05	336.8 ± 6.00			0.42 ± 0.02	14.80
$L_\infty = 418 \pm 13.47$	Gompertz	115	2256.48 ± 30.91	0	103.90 ± 2.17	359.19 ± 7.81		0.28 ± 0.01		14.19
Observed data (females)										
Hypothesis 1	VBGF	**165**	**2241.78 ± 29.57**	**1**	**101.58 ± 2.47**	**486.28 ± 14.71**	**0.11 ± 0.01**			**12.23**
$L_0 = 95$	Logistic	165	2287.57 ± 31.45	0	112.66 ± 2.56	381.26 ± 8.66			0.33 ± 0.02	13.78
$L_\infty = 526 \pm 17.72$	Gompertz	165	2260.67 ± 30.27	0	108.72 ± 2.54	416.49 ± 11.28		0.21 ± 0.01		12.96
Hypothesis 2	VBGF	**165**	**2235.37 ± 29.70**	**1**	**93.52 ± 2.39**	**401.21 ± 2.97**	**0.16 ± 0.00**			**12.56**
$L_0 = 95 \pm 3.15$	Logistic	165	2303.78 ± 28.42	0	114.63 ± 2.10	392.47 ± 3.07			0.31 ± 0.01	13.95
$L_\infty = 398.1 \pm 3.15$	Gompertz	165	2261.76 ± 29.98	0	105.77 ± 2.11	396.01 ± 2.96		0.23 ± 0.01		12.76
Back-calculated priors (females)										
Hypothesis 3	VBGF	**165**	**2241.45 ± 29.19**	**1**	**105.35 ± 1.33**	**496.49 ± 13.75**	**0.10 ± 0.01**			**12.16**
$L_0 = 104.50 \pm 1.43$	Logistic	165	2294.29 ± 32.23	0	108.50 ± 1.37	373.12 ± 6.75			0.35 ± 0.01	14.10
$L_\infty = 526 \pm 17.72$	Gompertz	165	2260.35 ± 30.44	0	107.48 ± 1.36	413.08 ± 9.42		0.21 ± 0.01		12.99

Note: The best-fitting Bayesian models are presented in bold.

Abbreviations: *g*, growth parameters for Log and Gom functions; *k*, the growth completion rate in $year^{-1}$ for the VBGF; L_0 ± SE, length-at-birth ± standard error (mm, TL); $L\infty$ ± SE, maximum asymptotic length ± standard error (mm, TL); LOOIC, leave-one-out cross-validation information criterion; *n*, number of sample; VBGF, von Bertalanffy's growth model; WLOOIC, LOOIC weights.

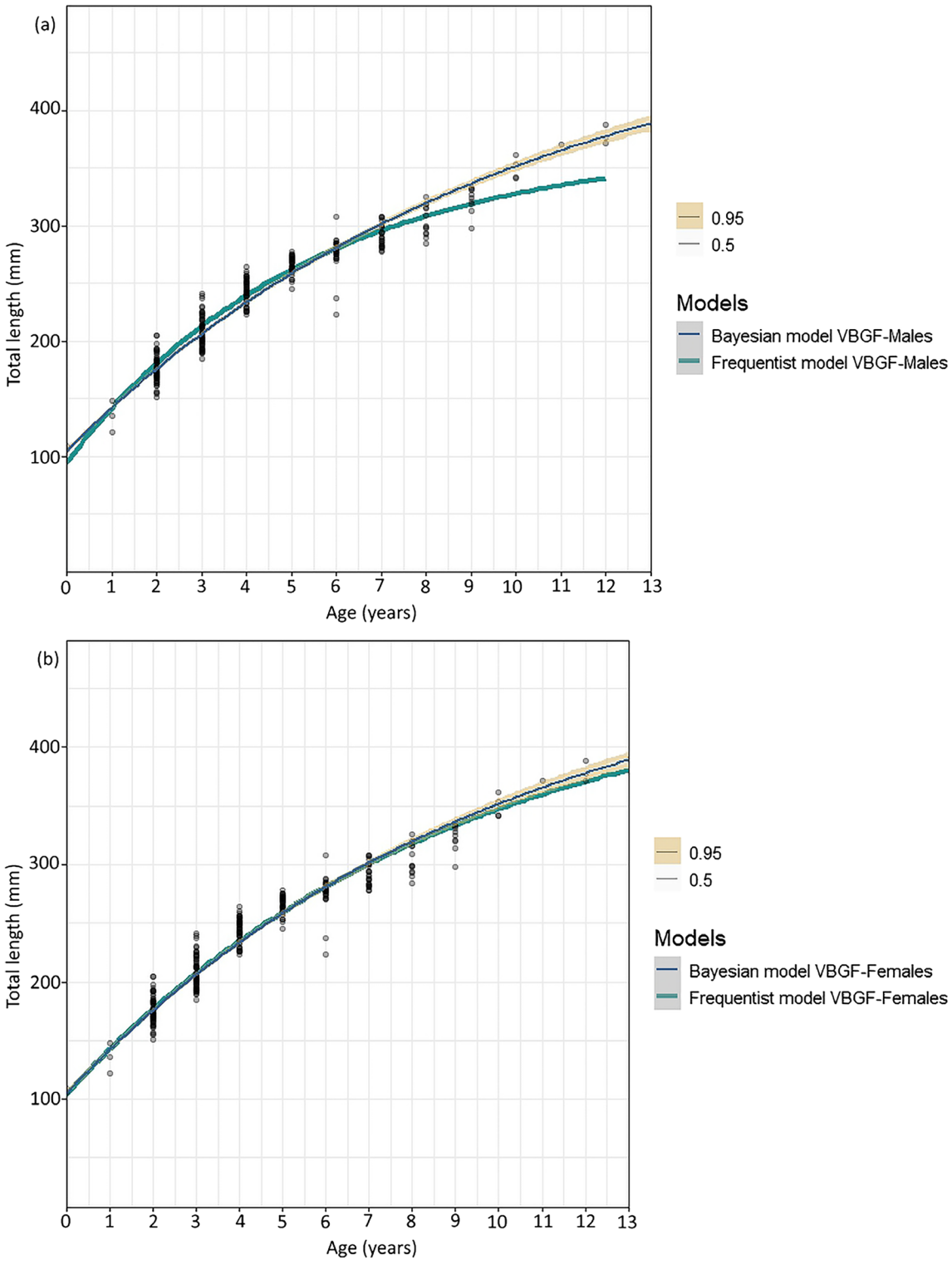

FIGURE 7 *Etmopterus molleri* growth curve in the East China Sea (ECS). (a) Males best-fitting Bayesian model [von Bertalanffy's growth model (VBGF)] (blue) with $L_0 = 101.88 \pm 2.12$ mm, $L_\infty = 397.70 \pm 10.21$ mm, $k = 0.15$ + best-fitting frequentist model VBGF (green) with $L_0 = 95 \pm 3.15$ mm, $L_\infty = 371.07 \pm 9.43$ mm, $k = 0.17$. (b) Females best-fitting Bayesian model VBGF (blue) with $L_0 = 105.35 \pm 1.33$ mm, $L_\infty = 496.49 \pm 13.75$ mm, $k = 0.10$ + best-fitting frequentist model VBGF (green with $L_0 = 104.26 \pm 4.46$ mm, $L_\infty = 463.40 \pm 21.76$ mm, $k = 0.14$).

catches can lead to long-term sustainability on the available stocks of this species in the ECS (Jørgensen et al., 2009; Pellowe & Leslie, 2020; Uusi-Heikkilä, 2020). Depth has been described as a significant factor in the distribution of deep-water shark species based on maturity stage; immature individuals are found in the upper water layers, where they reduce their mortality and increase their growth

Sex	L_{50} ± SE	L_{95} ± SE	A_{50} ± SE	A_{95} ± SE
Combined	269.37 ± 1.66	287.36 ± 3.36	5.38 ± 0.12	6.76 ± 0.25
Female	287.78 ± 4.19	320.44 ± 9.61	6.57 ± 0.18	7.62 ± 0.31
Male	261.28 ± 2.22	275.84 ± 3.86	4.77 ± 0.16	6.12 ± 0.32

TABLE 6 Summary of length and age-at-maturity analysis for *Etmopterus molleri* from East China Sea (ECS).

Note: L_{50} age (TL, mm) at 50% maturity, L_{95} age (TL, mm) at 95% and A_{50} age (years) at 50% maturity, A_{95} age (years) at 95% confidence interval (CI).

rates by reducing competition with adults (Riesgo et al., 2020), whereas the proportion of mature individuals increases with depth (Bottaro et al., 2023; Coelho & Erzini, 2010; Moura et al., 2014).

Although uterine fecundity assessment was limited by sample size, with only a single gravid female bearing one embryo, the absence of mature oocytes in this specimen suggests sequential rather than concurrent vitellogenesis and gestation in *E. molleri*. This reproductive pattern aligns with observations in *E. spinax* (Porcu et al., 2014; Kousteni, 2021) and other lecithotrophic species (Wheeler et al., 2024).

Furthermore, the length distribution displays a rather wide range, spanning from 106.5 to 389.1 mm for females and 121.1 to 371.1 mm for males. Females reached significantly larger sizes on average than males, which is common in many shark species due to sexual dimorphism related to reproduction (Gayford, 2023; Riesgo et al., 2020; Sims, 2005). A particularly interesting aspect of this study concerns the growth pattern observed in *E. molleri*, which displays isometric growth without significant difference between sexes. This could be due to the low representativeness of large individuals in the samples. This observation is relatively rare among sharks, which often exhibit allometric growth, representing adaptations to distinct ecological niches, as well as resource availability (Gayford, 2023; Irschick & Hammerschlag, 2014; Rigby & Simpfendorfer, 2015).

4.2 | Growth and age estimation

Vertebrae are among the most frequently utilized structures for age estimation in sharks. However, for small squalid sharks, their use is very limited, with several studies supporting the use of dorsal spines (Goldman et al., 2012; Natanson et al., 2018).

We used two histological staining techniques on whole vertebrae to overcome the age-reading issue. The first involved treatment with cobalt nitrate hexahydrate, whereas the second used alizarin red S. Although alizarin treatment is widely used for staining calcified structures (Irvine et al., 2006; Kindong et al., 2020; Oshitani et al., 2003), particularly due to its affinity with calcium ions, it does not seem suitable for weakly calcified vertebrae of deep-sea sharks, where it tends to infiltrate deeply into the vertebra, hindering the distinction of growth bands. Although a higher dilution (0.001%) was used compared to that indicated in the literature (Jolly et al., 2013; Kindong et al., 2020), the impregnation of the vertebrae with the solution did not allow for a clear distinction of the growth bands. Better results were obtained with the cobalt nitrate hexahydrate treatment, which offered the advantages of simplicity and rapidity, facilitated easier reading of growth bands under the microscope.

A significant proportion of vertebrae samples ($n = 234$) used for age determination had a perfect agreement between age estimates by readers. Proving that the technique was adequacy for the species and meet the accepted guidelines for elasmobranch age studies, requiring a CV <7.6% and an APE <5.5% (Cailliet & Goldman, 2004; Campana, 2001). This high precision in measurement could stem from the size range of individuals in the sample, which consisted of 69.64% immature individuals, as ageing error tends to increase with size (Campana, 2001; Harry, 2018). The study was unable to corroborate the periodicity of growth band formation, which was owing in part to a short sampling time that did not cover an extensive period, as well as the difficulties associated with typical validation approaches for deep-sea species (Caltabellotta et al., 2021; Irvine et al., 2006), and requires additional studies to confirm the estimated ages.

4.3 | Maturity

Unlike most bony fishes that reach maturity early (Okuzawa, 2002), shark species tend to exhibit delayed maturity, which can take several years or even decades, depending on the species. Contrary to general trends described in the literature, where most sharks reach sexual maturity at approximately 75% of their maximum length and 50% of their maximum age (Cortés, 2000; Pardo et al., 2013; Rigby et al., 2016), *E. molleri* was found to mature at small sizes compared to other congener deep-sea sharks. In comparison, both sexes of *Etmopterus bigelowi*, *E. spinax* and *E. pusillus* reach maturity between 75% and 87% of their maximum sizes (Aranha et al., 2009; Coelho & Erzini, 2005; Kousteni, 2021; Mourato et al., 2010). The same trend was reported for other deep-sea shark species such as *Centrophorus squamosus* and *Mitsukurina owstoni* (Clarke et al., 2002; Caltabellotta et al., 2018). Furthermore, studies have shown that females mature at significantly larger sizes than males. This pattern of sexual dimorphism in size at maturity is common among deep-water shark species (D'iglio et al., 2021; Rigby & Simpfendorfer, 2015).

4.4 | Comparison of growth models

Despite the reliable ageing process, the lack of small individuals in our sample limited the estimation of growth model parameters. To address this limitation, back-calculation of age-at-length from sampled

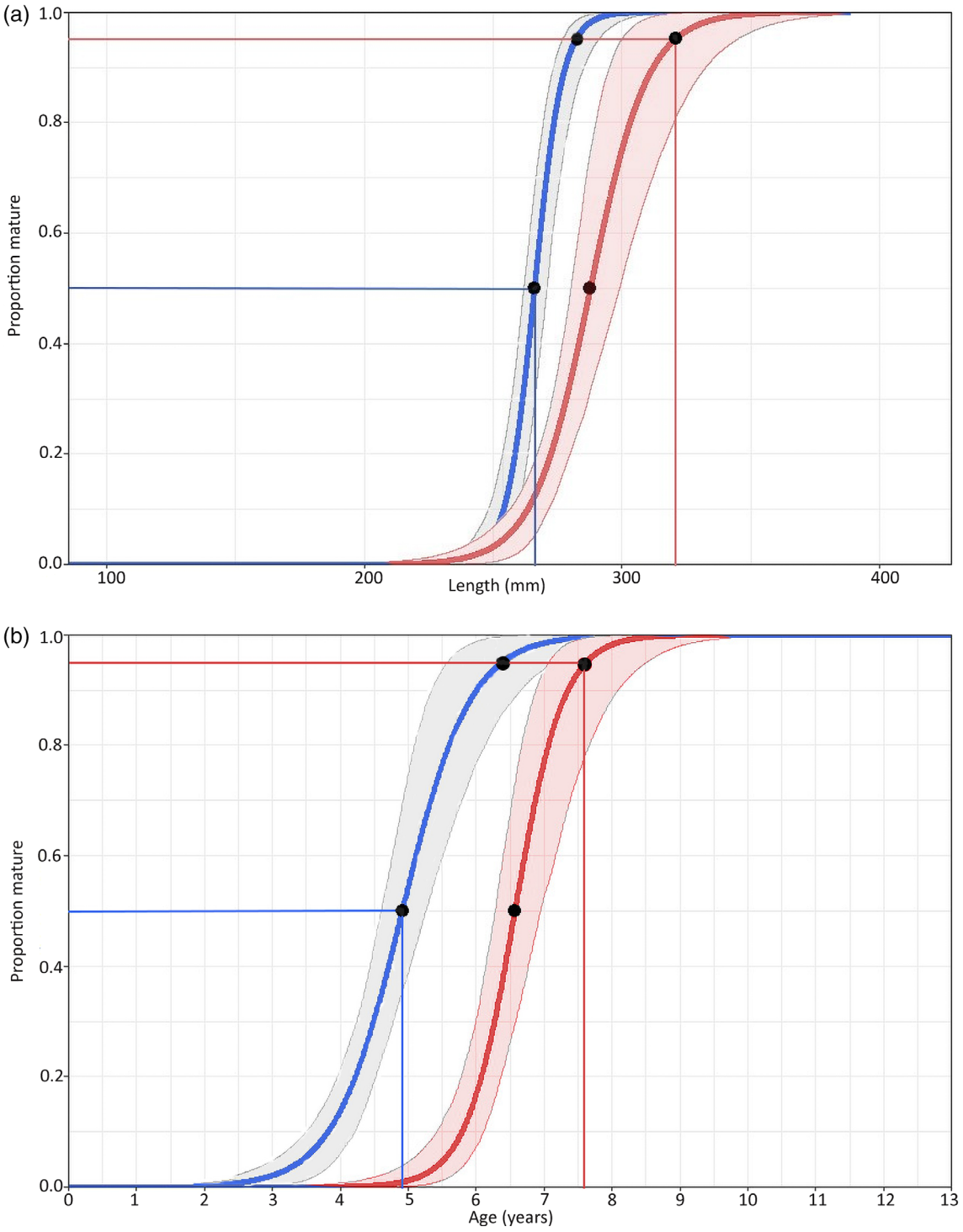

FIGURE 8 Maturity curves for *Etmopterus molleri*: (a) length-at-maturity and (b) age-at-maturity for males (blue) and females (red). In (a), the first black dot represents the length at 50% maturity, and the second represents the length at 95% maturity. In (b), the first black dot represents the age at 50% maturity, and the second represents the age at 95% maturity, respectively, for males ($n = 107$) and females ($n = 127$).

vertebrae enabled us to estimate birth size, which aligned with the minimum observed length in our dataset. The standard VBGF was found to be the best fit for growth parameters when the two sexes were looked at separately by both frequentist and Bayesian methods. Back-calculated and observed data had different assumptions for model selection, but estimates of birth sizes were the same for both sexes, averaging about 100 mm. This estimate was notably smaller than the 150 mm birth size reported for Australian waters (Ebert et al., 2013; Last & Stevens, 2009) and the minimum size of 123.4 mm documented for neonates of *E. molleri* in the ECS near Taiwanese waters (Joung & Chen, 1992). However, our estimate closely matched the smallest specimen (106.5 mm) observed in the present study.

Asymptotic lengths differed significantly between sexes across estimation models. Males' asymptotic lengths were close to the largest size seen in our dataset and in line with the longest lengths ever recorded in the sampling area (398 mm; Yano, 1988) and New Zealand waters (381.5 mm; Pinte et al., 2020) when best-fit models (both frequentist and Bayesian) were used with observed data. Back-calculated data, however, produced significantly larger values, though both estimates remained below the reported maximum species length of 460 mm (Ebert et al., 2013; Last & Stevens, 2009). For females, the frequentist model using observed data produced asymptotic lengths compared to literature values under various model assumptions, whereas back-calculated data yielded substantially larger estimates. The Bayesian model provided best fits for both birth size and asymptotic length estimates in females, although the latter exceeded maximum lengths reported in the literature (Ebert et al., 2013; Last & Stevens, 2009).

Although species-specific birth sizes were not explicitly documented, related species within the genus *Etmopterus* demonstrate comparable proportional birth sizes. *Etmopterus gracilispinis* exhibits birth lengths of 120–130 mm (Gianeti et al., 2009) representing approximately 34.29% of its maximum estimated length of 350 mm. Similarly, *E. spinax* shows birth sizes of 92.7 mm (Gennari & Scacco, 2007), approximately 20.21% of the female maximum estimated length of 480 mm. *E. molleri* displays a birth size ratio of 21.74% of its documented maximum length, which falls within the typical range for the genus *Etmopterus*.

Although frequentist and Bayesian growth modelling approaches reveal distinct methodologies and inherent advantages, studies have demonstrated that Bayesian modelling outperforms frequentist approaches in scenarios with biased or small sample sizes due to its ability to incorporate relevant biological information through priors (Fontez & Cavalli, 2014; Neves et al., 2022; Smart & Grammer, 2021). Although prior parameter selection can influence estimation accuracy (Smart & Grammer, 2021), the various scenarios considered in the Bayesian adjustment provided better growth parameter estimates for both sexes, aligning with back-calculated data, whereas the frequentist approach tended to overestimate asymptotic growth.

The growth completion rate for both approaches (Bayesian and frequentist growth model) corroborates that *E. molleri* seems to be vulnerable to fishing pressure (Andrade et al., 2019; Fernandez-Carvalho et al., 2011; Kyne & Simpfendorfer, 2010). Growth parameter estimates revealed distinct growth rates between sexes, with males exhibiting a higher growth coefficient ($k = 0.17$ year^{-1}) compared to females ($k = 0.11$ year^{-1}), indicating that males reach their maximum size more rapidly while females attain larger sizes. This sexual dimorphism is widespread among elasmobranchs, and the underlying drivers of size differences are complex, influenced by multiple selective pressures (Baje et al., 2018; Gayford, 2023). Although the 'fecundity advantage' model suggests that larger female size confers reproductive benefits (Pauly, 2019), in sharks, particularly lecithotrophic species, reproductive mode and ecological selection appear to play more significant roles than fecundity alone, differing from patterns observed in other vertebrates (Gayford & Sternes, 2024).

Like many other shark species inhabiting bathyal and abyssal environments, *E. molleri* is characterized by slow growth, a typical life-history trait of organisms adapted to oligotrophic conditions and resource scarcity in these deep ecosystems (Morato et al., 2006; Nehmens et al., 2021). This slow growth strategy, coupled with late maturity and generally low fecundity, confers on these species a limited demographic renewal capacity, making them particularly vulnerable to overexploitation, even when taken as by-catch (Dulvy et al., 2000; Stevens et al., 2000) due to their spatial overlap with the distribution of commercially important teleost species (Graça Aranha et al., 2023; Parra et al., 2016).

5 | CONCLUSION

This study addresses for the first time the blanks concerning the age and sexual maturity and redefines the growth parameters of one of the smallest but data-deficient sharks, *E. molleri*. Despite *E. molleri* vertebrae's low calcification, cobalt nitrate hexahydrate staining allowed for successful growth band reading. The combined use of frequentist and Bayesian approaches for growth modelling proved valuable, allowing the integration of available prior information and redefining the growth parameters. Our results provide critical insights into *E. molleri*, thereby establishing a crucial baseline for the development and refinement of future conservation strategies and management protocols. These data serve as a cornerstone for informed decision-making in efforts to protect and sustain this species.

AUTHOR CONTRIBUTIONS

Mboglen David: conceptualization, methodology, investigation, software, formal analysis, writing – original draft. Narcisse Ebango Ngando: formal analysis, writing – review and editing. Yongfu Shen: methodology, formal analysis. Yunkai Li: conceptualization, funding acquisition, resources, supervision, writing – review and editing. All authors provided editorial feedback and agreed that the manuscript should be submitted in this form.

ACKNOWLEDGEMENTS

This work was supported by the National Natural Science Foundation of China (no.: 42276092) and the Program for Professor of Special Appointment (Eastern Scholar) at Shanghai Institutions of Higher Learning. The authors thank the staff at Shanghai Ocean University for their assistance with sample collection and preparation, especially Dr. Richard Kindong.

FUNDING INFORMATION

This work was supported by the National Natural Science Foundation of China (no.: 42276092) and the Program for Professor of Special Appointment (Eastern Scholar) at Shanghai Institutions of Higher Learning.

CONFLICT OF INTEREST STATEMENT

The authors declare that they have no known competing financial interests or personal relationships that could have appeared to influence the work reported in this paper.

DATA AVAILABILITY STATEMENT

The raw data supporting the conclusions of this article will be made available by the authors, without undue reservation.

ORCID

Yunkai Li https://orcid.org/0000-0002-3686-1967

REFERENCES

Akhilesh, K. V., Anulekshmi, C., Bineesh, K. K., Ganga, U., & Pillai, N. G. K. (2020). Demographics of a heavily exploited deep-water shark Echinorhinus cf. brucus (Bonnaterre, 1788) from the south-eastern Arabian Sea. *Indian Journal of Fisheries*, *67*(1), 8–15. https://doi.org/10.21077/ijf.2019.67.1.92453-02

Andrade, I., Rosa, D., Muñoz-Lechuga, R., & Coelho, R. (2019). Age and growth of the blue shark (Prionace glauca) in the Indian Ocean. *Fisheries Research*, *211*, 238–246. https://doi.org/10.1016/j.fishres.2018.11.019

Aranha, A., Menezes, G., & Pinho, M. R. (2009). Biological aspects of the velvet belly lantern shark, Etmopterus spinax (Linnaeus, 1758) off the azores, north aast Atlantic. *Marine Biology Research*, *5*(3), 257–267. https://doi.org/10.1080/17451000802433175

Baje, L., Smart, J. J., Chin, A., White, W. T., & Simpfendorfer, C. A. (2018). Age, growth and maturity of the Australian sharpnose shark Rhizoprionodon taylori from the Gulf of Papua. *PLoS One*, *13*(10), e0206581. https://doi.org/10.1371/journal.pone.0206581

Beal, A. P., hackerott, S., Feldheim, K., Gruber, S. H., & Eirin-Lopez, J. M. (2022). Age group DNA methylation differences in lemon sharks (Negaprion brevirostris): Implications for future age estimation tools. *Ecology and Evolution*, *12*(8), e9226. https://doi.org/10.1002/ece3.9226

Bottari, T., Busalacchi, B., Profeta, A., Mancuso, M., Giordano, D., & Rinelli, P. (2014). Elasmobranch distribution and assemblages in the southern Tyrrhenian Sea (Central Mediterranean). *Journal of Aquaculture Research and Development*, *5*, 216. https://doi.org/10.4172/2155-9546.1000216

Bottaro, M., Sinopoli, M., Bertocci, I., Follesa, M. C., Cau, A., Consalvo, I., Scarcelli, F., Sperone, E., Vacchi, M., Marsili, L., Consales, G., & Danovaro, R. (2023). Jaws from the deep: Biological and ecological insights on the kitefin shark Dalatias licha from the Mediterranean Sea. *Frontiers in Marine Science*, *10*, 1155731. https://doi.org/10.3389/fmars.2023.1155731

Braccini, M., & Taylor, S. (2016). The spatial segregation patterns of sharks from Western Australia. *Royal Society Open Science*, *3*, 160306. https://doi.org/10.1098/rsos.160306

Burke, P. J., Raoult, V., Natanson, L. J., Murphy, T. D., Peddemors, V., & Williamson, J. E. (2020). Struggling with age: Common sawsharks (Pristiophorus cirratus) defy age determination using a range of traditional methods. *Fisheries Research*, *231*, 105706. https://doi.org/10.1016/j.fishres.2020.105706

Cailliet, G. M., & Goldman, K. J. (2004). Age determination and validation in chondrichthyan fishes. In *Biology of Sharks and Their Relatives* (pp. 399–448). CRC Press.

Cailliet, G. M., Smith, W. D., Mollet, H. F., & Goldman, K. J. (2006). Age and growth studies of chondrichthyan fishes: The need for consistency in terminology, verification, validation, and growth function fitting. *Environmental Biology of Fishes*, *77*, 211–228. https://doi.org/10.1007/s10641-006-9105-5

Caltabellotta, F. P., Silva, F. M., Motta, F. S., & Gadig, O. B. F. (2019). Age and growth of the threatened endemic skate rioraja agassizii (Chondrichthyes, Arhynchobatidae) in the western South Atlantic. *Marine and Freshwater Research*, *70*(1), 84–92. https://doi.org/10.1071/MF18010

Caltabellotta, F. P., Siders, Z. A., Cailliet, G. M., Motta, F. S., & Gadig, O. B. F. (2021). Preliminary age and growth of the deep-water goblin shark Mitsukurina owstoni (Jordan, 1898). *Marine and Freshwater Research*, *72*(3), 432–438. https://doi.org/10.1071/MF19370

Campana, S. E. (2001). Accuracy, precision and quality control in age determination, including a review of the use and abuse of age validation methods. *Journal of Fish Biology*, *59*(2), 197–242. https://doi.org/10.1006/jfbi.2001.1668

Campana, S. E., Ferretti, F., & Rosenberg, A. (2016). Sharks and Other Elasmobranchs. The First Global Integrated Marine Assessment, World Ocean Assessment I, 1437–1451. www.redlist.org

Clarke, M. W., Connolly, P. L., & Bracken†, J. J. (2002). Age estimation of the exploited deepwater shark centrophorus squamosus from the continental slopes of the rockall trough and porcupine bank. *Journal of Fish Biology*, *60*, 501–514.

Coelho, R., & Erzini, K. (2005). Length at first maturity of two species of lantern sharks (*Etmopterus spinax* and *Etmopterus pusillus*) off southern Portugal. *Journal of the Marine Biological Association of the United Kingdom*, *85*, 1163–1165.

Coelho, R., & Erzini, K. (2007). Population parameters of the smooth lantern shark, Etmopterus pusillus, in southern Portugal (NE Atlantic). *Fisheries Research*, *86*(1), 42–57. https://doi.org/10.1016/j.fishres.2007.04.006

Coelho, R., & Erzini, K. (2008a). Effects of fishing methods on deep-water shark species caught as by-catch off southern Portugal. *Hydrobiologia*, *606*(1), 187–193. https://doi.org/10.1007/s10750-008-9335-y

Coelho, R., & Erzini, K. (2008b). Life history of a wide-ranging deepwater lantern shark in the north-east Atlantic, Etmopterus spinax (Chondrichthyes: Etmopteridae), with implications for conservation. *Journal of Fish Biology*, *73*(6), 1419–1443. https://doi.org/10.1111/j.1095-8649.2008.02021.x

Coelho, R., & Erzini, K. (2010). Depth distribution of the velvet belly, Etmopterus spinax, in relation to growth and reproductive cycle: The case study of a deep-water lantern shark with a wide-ranging critical habitat. *Marine Biology Research*, *6*(4), 381–389. https://doi.org/10.1080/17451000802644706

Coiraton, C., Tovar-Ávila, J., Garcés-García, K. C., Rodríguez-Madrigal, J. A., Gallegos-Camacho, R., Chávez-Arrenquín, D. A., & Amezcua, F. (2019). Periodicity of the growth-band formation in vertebrae of juvenile scalloped hammerhead shark Sphyrna lewini from the Mexican Pacific Ocean. *Journal of Fish Biology*, *95*(4), 1072–1085. https://doi.org/10.1111/jfb.14100

Cortés, E. (1999). Standardized diet compositions and trophic levels of sharks. *ICES Journal of Marine Science*, *56*, 707–717.

Cortes, E. (2000). Life history patterns and correlations in sharks. *Reviews in Fisheries Science*, *8*(4), 299–344. https://doi.org/10.1080/10408340308951115

Council Regulation (EU) 2018/2025. (2018). fixing for 2019 and 2020 the fishing opportunities for Union fishing vessels for certain deep-sea fish stocks. http://data.europa.eu/eli/reg/2018/2025/oj

Council Regulation (EU) 2021/91. (2021). Fixing, for the years 2021 and 2022, the fishing opportunities for Union fishing vessels for certain deep-sea fish stocks. http://data.europa.eu/eli/reg/2021/91/oj

Croll, J. C., & van Kooten, T. (2022). Accounting for temporal and individual variation in the estimation of Von Bertalanffy growth curves. *Ecology and Evolution*, *12*, e9619. https://doi.org/10.1002/ece3.9619

D'iglio, C., Albano, M., Tiralongo, F., Famulari, S., Rinelli, P., Savoca, S., Spanò, N., & Capillo, G. (2021). Biological and ecological aspects of the blackmouth catshark (*Galeus melastomus* rafinesque, 1810) in the southern Tyrrhenian Sea. *Journal of Marine Science and Engineering*, *9*, 967. https://doi.org/10.3390/jmse9090967

Doll, J. C., & Lauer, T. E. (2013). Bayesian estimation of age and length at 50% maturity. *Transactions of the American Fisheries Society*, *142*(4), 1012–1024. https://doi.org/10.1080/00028487.2013.793615

Du, J., Ding, L., Su, S., Hu, W., Wang, Y., Loh, K. H., Yang, S., Chen, M., Roeroe, K. A., Songploy, S., Liu, Z., & Chen, B. (2022). Setting conservation priorities for marine sharks in China and the Association of Southeast Asian Nations (ASEAN) seas: What are the benefits of a 30% conservation target? *Frontiers in Marine Science*, *9*(933291), 933291. https://doi.org/10.3389/fmars.2022.933291

Duchatelet, L., Pinte, N., Tomita, T., Sato, K., & Mallefet, J. (2019). Etmopteridae bioluminescence: Dorsal pattern specificity and aposematic use. *Zoological Letters*, *5*(9), 9. https://doi.org/10.1186/s40851-019-0126-2

Dulvy, N. K., Fowler, S. L., Musick, J. A., Cavanagh, R. D., Kyne, P. M., Harrison, L. R., Carlson, J. K., Davidson, L. N., Fordham, S. V., Francis, M. P., Pollock, C. M., Simpfendorfer, C. A., Burgess, G. H., Carpenter, K. E., Compagno, L. J., Ebert, D. A., Gibson, C., Heupel, M. R., Livingstone, S. R., … White, W. T. (2014). Extinction risk and conservation of the world's sharks and rays. *eLife*, *3*, e00590. https://doi.org/10.7554/elife.00590

Dulvy, N. K., Metcalfe, J. D., Glanville, J., Pawson, M. G., & Reynolds, J. D. (2000). Fishery stability, local extinctions, and shifts in community structure in skates skate declines and community shifts Dulvy et al. *Conservation Biology*, *14*(1), 283–293.

Ebert, D. A., Fowler, S., & Compagno, L. (2013). *Sharks of the world*. Wild Nature Press.

Ebert, D. A., & Van Hees, K. E. (2018). *Etmopterus marshae* sp. nov., a new lanternshark (Squaliformes: Etmopteridae) from the Philippine Islands, with a revised key to the Etmopterus lucifer clade. *Zootaxa*, *4508*(2), 197–210. https://doi.org/10.11646/zootaxa.4508.2.3

Elliott, S. A. M., Carpentier, A., Feunteun, E., & Trancart, T. (2020). Distribution and life history trait models indicate vulnerability of skates. *Progress in Oceanography*, *181*, 102256. https://doi.org/10.1016/J.POCEAN.2019.102256

Fadool, B. A., Bostick, K. G., Brewster, L. R., Hansell, A. C., Carlson, J. K., & Smukall, M. J. (2024). Age and growth estimates for the nurse shark (*Ginglymostoma cirratum*) over 17 years in Bimini, The Bahamas. *Frontiers in Marine Science*, *11*(1265150), 1265150. https://doi.org/10.3389/fmars.2024.1265150

Feng, J. C., Liang, J., Cai, Y., Zhang, S., Xue, J., & Yang, Z. (2022). Deep-sea organisms research oriented by deep-sea technologies development. *Science Bulletin*, *67*(17), 1802–1816. https://doi.org/10.1016/J.SCIB.2022.07.016

Fernandez-Carvalho, J., Coelho, R., Erzini, K., & Neves Santos, M. (2011). Age and growth of the bigeye thresher shark, *Alopias superciliosus*, from the pelagic longline fisheries in the tropical northeastern Atlantic Ocean, determined by vertebral band counts. *Aquatic Living Resources*, *24*(4), 359–368. https://doi.org/10.1051/alr/2011046

Finucci, B., Cheok, J., Ebert, D. A., Herman, K., Kyne, P. M., & Dulvy, N. K. (2021). Ghosts of the deep – Biodiversity, fisheries, and extinction risk of ghost sharks. *Fish and Fisheries*, *22*(2), 391–412. https://doi.org/10.1111/faf.12526

Finucci, B., Pacoureau, N., Rigby, C. L., Matsushiba, J. H., Faure-Beaulieu, N., Sherman, C. S., VanderWright, W. J., Jabado, R. W., Charvet, P., Mejía-Falla, P. A., Navia, A. F., Derrick, D. H., Kyne, P. M., Pollom, R. A., Walls, R. H. L., Herman, K. B., Kinattumkara, B., Cotton, C. F., Cuevas, J.-M., … Dulvy, N. K. (2024). Fishing for oil and meat drives irreversible defaunation of deepwater sharks and rays. *Science*, *383*, 1135–1141. https://doi.org/10.1126/science.ade9121

Flinn, S. A., & Midway, S. R. (2021). Trends in growth modeling in fisheries science. *Fishes*, *6*(1), 1. https://doi.org/10.3390/fishes6010001

Fontez, B., & Cavalli, L. (2014). Bayesian hierarchical model used to analyze regression between fish body size and scale size: Application to rare fish species *Zingel asper*. *Knowledge and Management of Aquatic Ecosystems*, *413*(413), 10. https://doi.org/10.1051/kmae/2014008

Francis, M. P., & Ó Maolagáin, C. (2019). Growth-band counts from elephantfish *Callorhinchus milii* fin spines do not correspond with independently estimated ages. *Journal of Fish Biology*, *95*, 743–752. https://doi.org/10.1111/jfb.14060

Gayford, J. H. (2023). The evolution of sexual dimorphism in Chondrichthyes: Drivers, uncertainties, and future directions. *Environmental Biology of Fish*, *106*, 1463–1475. https://doi.org/10.1007/s10641-023-01425-x

Gayford, J. H., & Sternes, P. C. (2024). The origins and drivers of sexual size dimorphism in sharks. *Ecology and Evolution*, *14*, e11163. https://doi.org/10.1002/ece3.11163

Gennari, E., & Scacco, U. (2007). First age and growth estimates in the deep-water shark, Etmopterus Spinax (Linnaeus, 1758), by deep coned vertebral analysis. *Marine Biology*, *152*(5), 1207–1214. https://doi.org/10.1007/s00227-007-0769-y

Gervelis, B. J., & Natanson, L. J. (2013). Age and growth of the common thresher shark in the Western North Atlantic Ocean. *Transactions of the American Fisheries Society*, *142*(6), 1535–1545. https://doi.org/10.1080/00028487.2013.815658

Gianeti, M. D., Dias, J. F., & Vooren, C. M. (2009). Aspects of the population structure and reproductive biology of sharks of the genus Etmopterus on the upper continental slope of southern Brazil. *Marine Biodiversity Records*, *2*(e115), e115. https://doi.org/10.1017/s1755267209000967

Goldman, K. J., Cailliet, G. M., Andrews, A. H., & Natanson, L. J. (2012). Biology of sharks and their relatives. In *Assessing the age and growth of Chondrichthyan fishes* (2nd ed.). CRC Press; Taylor & Francis Group.

Graça Aranha, S., Dias, E., Marsili, T., Barkai, A., Queiroz, N., Pires da Rocha, P., & Teodósio, A. (2025). Unravelling the deep: Assessing the bycatch of deep-sea elasmobranchs in crustacean bottom trawl fisheries in Portugal. *Marine Policy*, *173*, 106555. https://doi.org/10.1016/j.marpol.2024.106555

Graça Aranha, S., Teodósio, A., Baptista, V., Erzini, K., & Dias, E. (2023). A glimpse into the trophic ecology of deep-water sharks in an important crustacean fishing ground. *Journal of Fish Biology*, *102*(3), 1–14. https://doi.org/10.1111/jfb.15306

Harry, A. V. (2018). Evidence for systemic age underestimation in shark and ray ageing studies. *Fish and Fisheries*, *00*, 1–16. https://doi.org/10.1111/faf.12243

Heupel, M. R., Knip, D. M., Simpfendorfer, C. A., & Dulvy, N. K. (2014). Sizing up the ecological role of sharks as predators. *Marine Ecology Progress Series*, *495*, 291–298. https://doi.org/10.3354/meps10597

Hilborn, R., & Walters, C. J. (1992). Quantitative fisheries stock assessment: Choice, dynamics, and uncertainty. *Review in Fish Biology and Fisheries*, *2*, 177–186.

Hoenig, J., & Brown, C. (1988). A simple technique for staining growth bands in elasmobranch vertebrae. *Bulletin of Marine Science*, *42*(2), 334–337.

Hooten, M. B., & Hobbs, N. T. (2015). A guide to Bayesian model selection for ecologists. *Ecological Society of America*, *85*, 3–28. https://doi.org/10.1890/14-0661.1

ICES. (2020). Workshop on the distribution and bycatch management options of listed deep-sea shark species (WKSHARK6). ICES Scientific Reports 2:76. 85 pp.

Irschick, D. J., & Hammerschlag, N. (2014). Morphological scaling of body form in four shark species differing in ecology and life history. *The Linnean Society of London, Biological Journal of the Linnean Society*, *114*, 126–135.

Irvine, S. B., Stevens, J. D., & Laurenson, L. J. B. (2006). Comparing external and internal dorsal-spine bands to interpret the age and growth of the giant lantern shark, Etmopterus baxteri (Squaliformes: Etmopteridae). *Environmental Biology of Fish*, *77*, 253–264. https://doi.org/10.1007/s10641-006-9130-4

Jiao, Y., Corte's, E., Andrews, K., Guo, F., Corté, E., & Guo, A. F. (2011). Poor-data and data-poor species stock assessment using a Bayesian hierarchical approach. *Ecological Applications*, *21*(7), 2691–2708.

Jolly, K., da Silva, C., & Attwood, C. (2013). Age, growth and reproductive biology of the blue shark Prionace glauca in south African waters. *African Journal of Marine Science*, *35*(1), 99–109. https://doi.org/10.2989/1814232X.2013.783233

Jørgensen, C., Ernande, B., & Fiksen, Ø. (2009). Size-selective fishing gear and life history evolution in the Northeast Arctic cod. *Evolutionary Applications*, *2*(3), 356–370. https://doi.org/10.1111/j.1752-4571.2009.00075.x

Joung, S.-J., & Chen, C.-T. (1992). The occurrence of two lanternsharks of the genus *Etmopterus* (*Squalidae*) in Taiwan. *Japanese Journal of Ichthyology*, *39*(1), 17–23.

Kim, J., Lee, S., Choi, I., Jeong, Y., & Woo, E. J. (2022). A comparative analysis of Bayesian age-at-death estimations using three different priors and Suchey-brooks standards. *Forensic Science International*, *336*, 111318. https://doi.org/10.1016/J.FORSCIINT.2022.111318

Kindong, R., Wang, H., Wu, F., Dai, X., & Tian, S. (2020). Age, growth, and sexual maturity of the crocodile shark, Pseudocarcharias kamoharai, from the eastern Atlantic Ocean. *Frontiers in Marine Science*, *7*, 586024. https://doi.org/10.3389/fmars.2020.586024

Kousteni, V. (2021). Shedding light on the deep: The case of the velvet belly lanternshark in the North Aegean Sea. *Journal of Fish Biology*, *99*(1), 101–117. https://doi.org/10.1111/jfb.14702

Kyne, P. M., Ebert, D. A., & Silva, S.-D. (2015). *Etmopterus molleri*. The IUCN Red List of threatened species 2015.

Kyne, P. M., & Simpfendorfer, C. A. (2010). Deepwater Chondrichthyans. In J. C. Carrier, J. A. Musick, & M. R. Heithaus (Eds.). Sharks and their relatives II.

Kyne, P. M., & Simpfendorfer, C. A. (2010). Deepwater Chondrichthyans. In *Sharks and their relatives II: Biodiversity, adaptive physiology, and conservation* (pp. 37–113). CRC Press; Taylor & Francis Group.

Last, P. R., & Stevens, J. D. (2009). *Sharks and rays of Australia* (2nd ed.). CSIRO Publishing.

Matta, M. E., Tribuzio, C. A., Ebert, D. A., Goldman, K. J., & Gburski, C. M. (2017). Age and growth of elasmobranchs and applications to fisheries management and conservation in the Northeast Pacific Ocean. *Advances in Marine Biology*, *7*, 179–220.

Melis, R., Vacca, L., Cariani, A., Carugati, L., Cau, A., Charilaou, C., Di Crescenzo, S., Ferrari, A., Follesa, M. C., Hemida, F., Helyar, S., Lo Brutto, S., Sion, L., Tinti, F., & Cannas, R. (2023). Commercial sharks under scrutiny: Baseline genetic distinctiveness supports structured populations of small-spotted catsharks in the Mediterranean Sea. *Frontiers in Marine Science*, *10*, 1050055. https://doi.org/10.3389/fmars.2023.1050055

Morato, T., Watson, R., Pitcher, T. J., & Pauly, D. (2006). Fishing down the deep. *Fish and Fisheries*, *7*, 24–34.

Moura, T., Jones, E., Clarke, M. W., Cotton, C. F., Crozier, P., Daley, R. K., Diez, G., Dobby, H., Dyb, J. E., Fossen, I., Irvine, S. B., Jakobsdottir, K., López-Abellán, L. J., Lorance, P., Pascual-Alayón, P., Severino, R. B., & Figueiredo, I. (2014). Large-scale distribution of three deep-water squaloid sharks: Integrating data on sex, maturity and environment. *Fisheries Research*, *157*, 47–61.

Mourato, B. L., Coelho, R., Amorim, A. F., Carvalho, F. C., Hazin, F. H. V., & Burgess, G. (2010). Size at maturity and length-weight relationships of the blurred lanternshark *Etmopterus bigelowi* (Squaliformes: Etmopteridae) caught off southeastern Brazil. *Ciencias Marinas*, *36*(4), 323–331. https://doi.org/10.7773/cm.v36i4.1723

Myers, R. A., & Worm, B. (2005). Extinction, survival or recovery of large predatory fishes. *Philosophical Transactions of the Royal Society B*, *360*, 13–20. https://doi.org/10.1098/rstb.2004.1573

Natanson, L. J., Skomal, G. B., Hoffmann, S. L., Porter, M. E., Goldman, K. J., & Serra, D. (2018). Age and growth of sharks: Do vertebral band pairs record age? *Marine and Freshwater Research*, *69*(9), 1440–1452. https://doi.org/10.1071/MF17279

Nehmens, M. C., Varney, R. M., Janosik, A. M., & Ebert, D. A. (2021). An exploratory study of telomere length in the Deep-Sea shark, *Etmopterus granulosus*. *Frontiers in Marine Science*, *8*, 642872. https://doi.org/10.3389/fmars.2021.642872

Neves, A., Vieira, A. R., Sequeira, V., Silva, E., Silva, F., Duarte, A. M., Mendes, S., Ganhão, R., Assis, C., Rebelo, R., Magalhães, M. F., Gil, M. M., & Gordo, L. S. (2022). Modelling fish growth with imperfect data: The case of *Trachurus picturatus*. *Fishes*, *7*(1), 52. https://doi.org/10.3390/fishes7010052

Ogle, D., Doll, J., Wheeler, A., & Dinno, A. (2023). FSA: Simple Fisheries Stock Assessment Methods. R package version 0.9.5. https://fishr-core-team.github.io/FSA/

Ogle, D. H. (2023). RFishBC: Back-Calculation of Fish Length. R package version 0.2.7. https://fishr-core-team.github.io/RFishBC/

O'Hea, B., Davie, S., Johnston, G., & O'Dowd, L. (2020). Assemblages of deepwater shark species along the north east Atlantic continental slope. *Deep-Sea Research Part I: Oceanographic Research Papers*, *157*, 103207. https://doi.org/10.1016/j.dsr.2019.103207

Okuzawa, K. (2002). Puberty in teleosts. *Fish Physiology and Biochemistry*, *26*, 31–41.

Oshitani, S., Nakano, H., & Tanaka, S. (2003). Age and growth of the silky shark Carcharhinus falciformis from the Pacific Ocean. *Fisheries Science*, *69*, 456–464. https://doi.org/10.1046/j.0919-9268.2003.00645.x

Pardo, S. A., Cooper, A. B., & Dulvy, N. K. (2013). Avoiding fishy growth curves. *Methods in Ecology and Evolution*, *4*, 353–360. https://doi.org/10.1111/2041-210x.12020

Pardo, S. A., Kindsvater, H. K., Cuevas-Zimbrón, E., Sosa-Nishizaki, O., Pérez-Jiménez, J. C., & Dulvy, N. K. (2016). Growth, productivity, and relative extinction risk of a data-sparse devil ray. *Scientific Reports*, *6*, 33745. https://doi.org/10.1038/srep33745

Parra, H. E., Pham, C. K., Menezes, G. M., Rosa, A., Tempera, F., Morato, T., & Parra, H. (2016). Predictive modelling of deep-sea fish distribution in the Azores. *Deep Sea Research Part II: Topical Studies in Oceanography*, *145*, 49–60. https://doi.org/10.1016/j.dsr2.2016.01.004

Pauly, D. (1983). Some simple methods for the assessment of tropical fish stocks. FAO Fish Technical Paper, 234, 52 p.

Pauly, D. (2019). Female fish grow bigger – Let's Deal with it. *Trends in Ecology and Evolution*, *34*(3), 181–182. https://doi.org/10.1016/j.tree.2018.12.007

Pellowe, K. E., & Leslie, H. M. (2020). Size-selective fishing leads to trade-offs between fishery productivity and reproductive capacity. *Ecosphere*, *11*(3), e03071. https://doi.org/10.1002/ecs2.3071

Pinte, N., Coubris, C., Jones, E., & Mallefet, J. (2021). Red and white muscle proportions and enzyme activities in mesopelagic sharks. *Comparative Biochemistry and Physiology Part B: Biochemistry & Molecular Biology*, *256*, 110649. https://doi.org/10.1016/j.cbpb.2021.110649

Pinte, N., Godefroid, M., Abbas, O., Baeten, V., & Mallefet, J. (2019). Deep-sea sharks: Relation between the liver's buoyancy and red aerobic muscle volumes, a new approach. *Comparative Biochemistry and Physiology -Part A*, *236*, 110520. https://doi.org/10.1016/j.cbpa.2019.06.020

Pinte, N., Parisot, P., Martin, U., Zintzen, V., De Vleeschouwer, C., Roberts, C. D., & Mallefet, J. (2020). Ecological features and swimming capabilities of deep-sea sharks from New Zealand. *Deep-Sea Research Part I: Oceanographic Research Papers*, *156*, 103187. https://doi.org/10.1016/j.dsr.2019.103187

Porcu, C., Marongiu, M. F., Follesa, M. C., Bellodi, A., Mulas, A., Pesci, P., & Cau, A. (2014). Reproductive aspects of the velvet belly *Etmopterus spinax* (Chondrichthyes: Etmopteridae), from the central western Mediterranean Sea. Notes on gametogenesis and oviducal gland microstructure. *Mediterranean Marine Science*, *15*(2), 313–326. https://doi.org/10.12681/mms.559

Pratt, H. L. (1979). Reproduction in the blue shark, *Prionace glauca*. *Fishery Bulletin*, *77*(2), 445–470.

Punt, A. E., & Hilborn, R. (1997). Fisheries stock assessment and decision analysis: The Bayesian approach. *Reviews in Fish Biology and Fisheries*, *7*, 35–63.

Riesgo, L., Cortes, M. A., Velasco, F., & Baldó, F. (2020). Evidence of sexual segregation in a common deep-sea shark: implications for conservation and management. VII International Symposium on Marine Sciences, 110, Barcelona (Spain), 1st-3rd July 2020.

Rigby, C., & Simpfendorfer, C. A. (2015). Patterns in life history traits of deep-water chondrichthyans. *Deep-Sea Research Part II*, *115*, 30–40. https://doi.org/10.1016/j.dsr2.2013.09.004

Rigby, C. L., White, W. T., Smart, J. J., & Simpfendorfer, C. A. (2016). Life histories of two deep-water Australian endemic elasmobranchs: Argus skate dipturus polyommata and eastern spotted gummy shark mustelus walkeri. *Journal of Fish Biology*, *88*, 1149–1174.

Rodríguez-Cabello, C., González-Pola, C., Rodríguez, A., & Sánchez, F. (2018). Insights about depth distribution, occurrence and swimming behavior of Hexanchus griseus in the Cantabrian Sea (NE Atlantic). *Regional Studies in Marine Science*, *23*, 60–72. https://doi.org/10.1016/J.RSMA.2017.10.015

Rodríguez-Cabello, C., & Sánchez, F. (2017). Catch and post-release mortalities of deep-water sharks caught by bottom longlines in the Cantabrian Sea (NE Atlantic). *Journal of Sea Research*, *130*, 248–255. https://doi.org/10.1016/j.seares.2017.04.004

Ruibal Núñez, J., Bovcon, N. D., Cochia, P. D., & Góngora, M. E. (2018). Bycatch of chondrichthyans in a coastal trawl fishery on Chubut province coast and adjacent waters, Argentina. *Journal of the Marine Biological Association of the United Kingdom*, *98*(3), 605–616. https://doi.org/10.1017/S0025315416001508

Simpfendorfer, C., & Kyne, P. M. (2009). Limited potential to recover from overfishing raises concerns for deep-sea sharks, rays and chimaeras. *Environmental Conservation*, *36*(02), 97–103. https://doi.org/10.1017/S0376892909990191

Sims, D. W. (2005). Sexual segregation in vertebrates. In K. Ruckstuhl & P. Neuhaus (Eds.), *Differences in habitat selection and reproductive strategies of male and female sharks*. Cambridge University Press.

Smart, J. J., Chin, A., Tobin, A. J., & Simpfendorfer, C. A. (2016). Multimodel approaches in shark and ray growth studies: Strengths, weaknesses and the future. *Fish and Fisheries*, *17*(4), 955–971. https://doi.org/10.1111/faf.12154

Smart, J. J., & Grammer, G. L. (2021). Modernising fish and shark growth curves with Bayesian length-at-age models. *PLoS One*, *16*(2), e0246734. https://doi.org/10.1371/journal.pone.0246734

Smith, W. D., Miller, J. A., & Heppell, S. S. (2013). Elemental markers in elasmobranchs: Effects of environmental history and growth on vertebral chemistry. *PLoS One*, *8*(10), 62423. https://doi.org/10.1371/journal.pone.0062423

Stehmann, M. F. W. (2002). Proposal of a maturity stages scale for oviparous and viviparous cartilaginous fishes (Pisces, Chondrichthyes). *Archive of Fishery and Marine Research*, *50*(1), 23–48.

Stevens, J. D., Bonfil, R., Dulvy, N. K., & Walker, P. A. (2000). The effects of fishing on sharks, rays, and chimaeras (chondrichthyans), and the implications for marine ecosystems. *ICES Journal of Marine Science*, *57*, 476–494. https://doi.org/10.1006/jmsc.2000.0724

Uusi-Heikkilä, S. (2020). Implications of size-selective fisheries on sexual selection. *Evolutionary Applications*, *13*, 1487–1500. https://doi.org/10.1111/eva.12988

Victorero, L., Watling, L., Palomares, M. L. D., & Nouvian, C. (2018). Out of sight, but within reach: A global history of bottom-trawled deep-sea fisheries from >400 m depth. *Frontiers in Marine Science*, *5*, 98. https://doi.org/10.3389/fmars.2018.00098

Wheeler, C. R., Anderson, B. N., Campbell, B., Sulikowski, J. A., & Awruch, C. (2024). Unique aspects of reproductive energetics and endocrinology among Chondrichthyes. In Sarah L. Alderman & Todd E. Gills (Eds.), *Encyclopedia of Fish Physiology* (Second edition, pp. 357–367). Academic Press. https://doi.org/10.1016/B978-0-323-90801-6.00160-9

Wong, D., Smart, J. J., Barrow, J., Cleeland, J., Yates, P., Ziegler, P., & Rizzari, J. R. (2022). Age, growth and maturity of Southern Ocean skates (*Bathyraja* spp.) from the Kerguelen plateau. *Polar Biology*, *45*(6), 1119–1130. https://doi.org/10.1007/s00300-022-03062-z

Wu, F., Kindong, R., Dai, X., Sarr, O., Zhu, J., Tian, S., Li, Y., & Nsangue, B. T. N. (2020). Aspects of the reproductive biology of two pelagic sharks in the eastern Atlantic Ocean. *Journal of Fish Biology*, *97*(6), 1651–1661. https://doi.org/10.1111/jfb.14526

Xu, Y., Dai, X., Huang, Z., Sun, M., Chen, Z., & Zhang, K. (2022). Stock assessment of four dominant shark bycatch species in bottom trawl fisheries in the northern South China Sea. *Sustainability*, *14*, 3722. https://doi.org/10.3390/su14073722

Yano, K. (1988). A new Lanternshark *Etmopterus splendidus* from the East China Sea and Java Sea. *Japanese Journal of Ichthyology*, *34*(4), 421–425.

Zar, J. H. (1999). *Biostatistical analysis* (4th ed.). Prentice Hall.

Zhang, S., Jin, S., Zhang, H., Fan, W., Tang, F., & Yang, S. (2016). Distribution of bottom trawling effort in the Yellow Sea and East China Sea. *PLoS One*, *11*(11), e0166640. https://doi.org/10.1371/journal.pone.0166640

SUPPORTING INFORMATION

Additional supporting information can be found online in the Supporting Information section at the end of this article.

How to cite this article: David, M., Ebango Ngando, N., Shen, Y., & Li, Y. (2025). Deciphering age, growth and maturity patterns in one of the smallest but data-deficient shark species, slendertail lanternshark (*Etmopterus molleri*), from the East China Sea. *Journal of Fish Biology*, 1–20. https://doi.org/10.1111/jfb.70074